Author Manuscript

Author Manuscript

Author Manuscript

Author Manuscript

HHS Public Access

Author manuscript

J Am Chem Soc. Author manuscript; available in PMC 2020 June 12.

Published in final edited form as:

J Am Chem Soc. 2019 June 12; 141(23): 9106–9123. doi:10.1021/jacs.9b03337.

Enabling Two-Electron Pathways with Iron and Cobalt: From Ligand Design to Catalytic Applications.

Rebeca Arevalo and **Paul J. Chirik**

Department of Chemistry, Princeton University, Princeton, New Jersey 08544, United States

Abstract

Homogeneous catalysis with Earth-abundant, first-row transition metals, including iron and cobalt, has gained considerable recent attention as a potentially cost-effective and sustainable alternative to more commonly and historically used precious metals. Because fundamental organometallic transformations, such as oxidative addition and reductive elimination, are two-electron processes and essential steps in many important catalytic cycles, controlling redox chemistry, in particular overcoming one-electron chemistry, has been as a central challenge with Earth-abundant metals. This Perspective focuses on approaches to impart sufficiently strong-ligand fields to generate electron-rich metal complexes able to promote oxidative addition reactions where the redox changes are exclusively metal-based. Emphasis is placed on how ligand design and exploration of fundamental organometallic chemistry coupled with mechanistic understanding has been used to discover iron catalysts for the hydrogen isotope exchange in pharmaceuticals and cobalt catalysts for C(sp^2)—H borylation reactions. A pervasive theme is that first-row metal complexes often promote unique chemistry from their precious-metal counterparts, demonstrating that these elements offer a host of new opportunities for reaction discovery and for sustainable catalysis.

Graphical Abstract

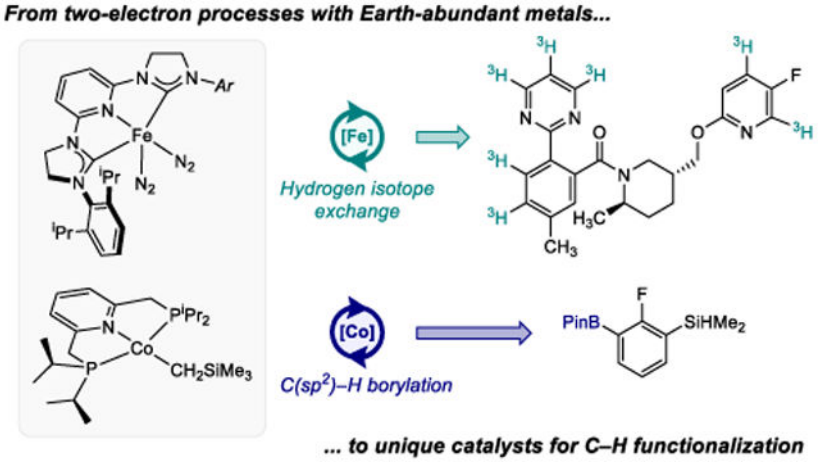

Corresponding Author pchirik@princeton.edu.

Notes

The authors declare no competing financial interests.

Author Manuscript Author Manuscript Author Manuscript Author Manuscript

Introduction.

Two-electron processes are at the heart of organometallic chemistry and homogeneous catalysis with transition metals. Oxidative addition and its microscopic reverse, reductive elimination, are key bond-activation and product-forming steps, respectively, in many catalytic cycles.[1] These transformations have generally been the provenance of late second- and third-row transition metals supported by strong field cyclopentadienyl, phosphine, *N*-heterocyclic carbene and related ligands. As interest in first-row metal catalysis continues to grow,[2,3,4] so does interest in using relatively Earth-abundant, first-row transition metals as alternatives to precious ones in catalytic reactions.[5] Key to realizing this goal is enabling two-electron redox chemistry with 3d transition metals in lieu of one-electron alternatives.[6]

Several strategies have been developed to enable two-electron redox-chemistry and, hence, fundamental organometallic reactivity relevant to homogeneous catalysis with first-row transition metals such as iron and cobalt. One approach involves *electronic* metal-ligand cooperativity (Scheme 1a),[7] whereby a redox-active ligand, one that undergoes reversible electron transfer with the transition metal,[8] participates in redox chemistry during a chemical transformation. A second is *chemical* metal-ligand cooperativity (Scheme 1b) whereby a supporting ligand engages in reversible bond-making and -breaking events during catalytic turnover.[9] A third possibility is metal-metal cooperativity (Scheme 1c) which takes advantage of the ability of two metals in multimetallic complexes to undergo a one-electron redox event rendering a net two-electron process.[10]

An illustrative example of electronic metal-ligand cooperativity is the C—C oxidative addition of biphenylene to the pyridine(diimine) iron dinitrogen complex, (^{iPr}PDI)FeN_2 (^{iPr}PDI = 2,6-(2,6-^{i}Pr$_2$-C_6H_3N=CMe)$_2$$C_5H_3$N; Scheme 1a).[7] Combined spectroscopic, magnetic and computational data support two-electron oxidation of the intermediate-spin iron(II) dinitrogen complex with a diradical, dianionic ligand to an iron(III) derivative with a one-electron reduced pyridine(diimine) radical. Additional insights into the mechanism of this transformation demonstrate the cooperative redox behavior where both the metal and the chelate are concomitantly oxidized by one electron. Cooperative metal-ligand oxidative addition has been recently computed by Cundari and coworkers[11] for the oxidative addition of B—B bonds, a key step during the pyridine(diimine) cobalt-catalyzed 1,1-diboration of alkynes.[12]

It is possible that with the appropriate ligand field, low- spin complexes would be preferred, and the resulting metal complexes would be sufficiently reducing to promote exclusively metal-based oxidative addition (Scheme 1d). As will be highlighted in this Perspective, this strategy has been known in stoichiometric chemistry and in some instances, found to be key for C—H functionalization. However, general principles for rational catalyst design have been lacking. Here we describe the evolution of iron and cobalt complexes to enable the two-electron, metal-based oxidative addition of polar and non-polar bonds that ultimately has resulted in new catalytic chemistry using Earth-abundant first-row metals. Emphasis is placed on reactivity and transformations available with iron and cobalt distinct from precious metals.

Author Manuscript Author Manuscript Author Manuscript Author Manuscript

Historical Perspective.

Given the long-standing importance of iron in organometallic chemistry, it is perhaps unsurprising that two-electron oxidative addition reactivity has been known with this metal for some time. In fact, observation of intramolecular C(sp^2)—H oxidative addition to reduced iron[13] pre-dates the well-known iridium examples often cited as launching the field.[14,15] Ittel, Tolman and coworkers[16,17,18] at DuPont explored the intermolecular oxidative addition chemistry of C—H bonds employing six-coordinate Fe(0) or Fe(II) complexes. Specifically, the iron(0) alkene complex, (dppe)2Fe(η^2-CH_2=CH_2)[16] (dppe = 1,2-bis(diphenylphosphino)ethane), and the iron(II) precursors (dppe)$_2$FeMe$_2$,[17] (dppe)$_2$FeH$_2$[17] and (dmpe)$_2$FeH(Np)[18] (dmpe = 1,2-bis(dimethylphosphino)ethane, Np = 2-naphthyl) were effective for the C—H cleavage of arenes (Scheme 2a), alkenes, alkynes, and the C(sp^3)—H bond of cyclopentadiene.

The relevance of these observations to C—H oxidative addition was established by Field and coworkers who demonstrated that the 16 electron, iron(0) intermediate, (dmpe)$_2$Fe, was generated photochemically from (dmpe)$_2$FeH$_2$ and promotes the cleavage of C(sp^3)—H bonds in pentane and methane.[19] These observations support (dmpe)$_2$Fe as a common intermediate for C—H activation that can be accessed either by reductive elimination from iron(II) precursors or by olefin dissociation from (dppe)$_2$Fe(η^2-CH_2=CH2).

Although (dmpe)$_2$Fe has been known for over three decades to promote the stoichiometric activation of carbon-hydrogen bonds,[16,17,18] it was not until 2015 that reactions of this type were rendered catalytic. Bontemps, Sortais, Sabo-Etienne, Darcel and coworkers reported the application of the iron(II) derivatives, (dmpe)$_2$FeH$_2$ and (dmpe)$_2$FeMe$_2$ as precatalysts for the borylation of C(sp^2)—H bonds of arenes and furans with HBPin (Pin = pinacolate) under UV irradiation (Scheme 2b).[20] Iron (II) complexes containing cyclopentadienyl ligands have been also successfully employed for stoichiometric[21] and catalytic borylation,[10,22] although in these cases C—H activation is believed to occur by σ-bond metathesis rather than oxidative addition.[23] A particularly noteworthy example was provided by Mankad and coworkers who demonstrated that the bimetallic complex, Cp(CO)$_2$Fe-Cu(IPr) (IPr = *N,N′*-bis(2,6-diisopropylphenyl)imidazol-2-ylidene) was active for catalytic borylation of arenes upon irradiation with UV light.[10a] Although C—H activation occurs by σ-bond metathesis on the monometallic complex CpFe(CO)$_2$(BPin), oxidative addition of HBPin and reductive elimination of H_2 proceeds by 2-electron processes enabled by Fe-Cu cooperativity (Scheme 1c).[10b]

Oxidative addition by iron(0) precursors was also studied by Jones and coworkers in the context of the catalytic synthesis of aromatic aldimines.[24] Irradiation of Fe(PMe_3)$_2$(CNR)$_3$ (R = Me, *t*Bu, CH_2CMe_3, Ph and 2,6-xylyl) with UV light resulted in loss of an isocyanide ligand to generate the 16-electron Fe(PMe)$_2$(CNR)$_2$ intermediate, which is proposed to promote the oxidative addition of the C(sp^2)—H bond. While the scope of the reaction was only demonstrated for benzene and toluene, this nevertheless was an important advance in C—H functionalization with Earth-abundant transition metals. RauchfUss and coworkers have also reported the oxidative addition of a diphosphine anhydride to iron carbonyl precursors as a ligand metallation approach.[25] More recently, Furstner and coworkers have

Author Manuscript Author Manuscript Author Manuscript Author Manuscript

reported that the phosphine supported iron(0) alkene complex (dippp)Fe(C_2H_4)$_2$ (dippp = bis(diisopropylphosphino)propane) promotes the activation of the allylic C(sp^3)—H allylic bonds of 1,3-cyclohexadiene initiating a cascade of C-H activation events ultimately yielding the iron(II) complex (dippp)FeH(η^5-C_8H_{11}).[26] The formally 18-electron, cationic cobalt precursor, [(depe)$_2$Co(η^2-CS_2)]BPh_4 (depe = 1,2-bis(diethylphosphino)ethane) also promotes similar C—H oxidative addition chemistry (Scheme 3a).[27] Following dissociation of the CS_2 ligand, the putative 16 electron cobalt(I) intermediate, [(depe)$_2$Co]$^+$, promotes the oxidative addition of alkyne C—H bonds to generate the *trans*-alkynyl hydride cobalt(III) product. Brookhart and coworkers have also reported the synthesis of (η^5-C_5Me_5)Co(η^2-CH_2=CHR)$_2$ and the H—D exchange reactivity between benzene or toluene and the vinylic hydrogens of the coordinated alkenes (Scheme 3b).[28] Kinetic data support a mechanism involving reversible dissociation of an alkene to generate the 16-electron, cobalt(I) intermediate (η^5-C_5Me_5)Co(η^2-CH_2=CHR), responsible for rate-determining C—H(D) oxidative addition. This cobalt derivative was also effective for the cleavage of C—H bonds of aldehydes and the C(sp^3)—H bonds of amines, and, has also been employed for catalytic hydroacylation of alkenes (Scheme 3c),[29] and for catalytic transfer dehydrogenation to yield enamines.[30]

While cobalt (III) complexes from C—H oxidative addition to (η^5-C_5Me_5)Co(η^2-CH_2=CHR) are key intermediates in the C—H functionalization reactions catalyzed by this complex, their isolation remains elusive. In fact, it has not been until recently that Perez-Temprano and coworkers have been able to isolate and fully characterize the cobalt (III) iodide derivative, (η^5-C_5Me_5)CoI(ppy) (ppy = 2-phenylpyridine), from C—I oxidative addition of 2-(2-iodophenyl)pyridine (Scheme 3b, bottom).[31]

Fundamental studies aiming to understand and, ultimately, promote reductive elimination from iron complexes are remain scarce especially when compared to the number of studies for the microscopic reverse, oxidative addition. The few reported cases focus on C—C reductive elimination primarly due to its relevance in C—C cross-coupling reactions. Seminal work by Kochi and coworkers explored the role of the iron oxidation state on reductive elimination from the dialkyl iron compounds (bipy)$_2$Fe(CH_2CH_3)$_2$ and (bipy)$_2$Fe(CH_2)$_4$ (bipy = 2,2'-bipyridine).[32] These studies support that reductive elimination is the preferred pathway for iron(IV) compounds, while iron(II) and (III) undergo preferentially β-hydrogen elimination and radical ejection, respectively. More recently, our group h as investigated related phenthroline derivatives and what role exogeneous ligands play in C-C reductive elimination in Kochi-type compounds. The neutral ferracyclopentane complex, (phen)$_2$Fe(CH_2)$_4$ (phen = 1,10-phenanthroline), only underwent C—C reductive elimination upon treatment with strong π-accepting ligands, including CO, maleic anhydride and *p*-benzoquinone. In the presence of CO, reductive elimination presumably proceeds from the putative six-coordinate iron(II) complex Fe(CO)$_4$(CH_2)$_4$ (Scheme 4a), hinting that the presence of CO ligands renders a more oxidized iron center that preferentially undergoes reductive elimination over radical ejection or β-hydrogen elimination.[33]

As with iron, understanding the fundamental aspects of reductive elimination from cobalt complexes remains underexplored. Reductive elimination of ethane from the cobalt (III) complex CoI(CH_3)$_2$(PMe_3)$_3$ under thermal conditions has been reported by Bernskoetter

Author Manuscript Author Manuscript Author Manuscript Author Manuscript

and coworkers.[34] Mechanistic investigations support that reductive elimination occurs from a 5-coordinate cobalt complex formed upon PMe_3 loss (Scheme 4b), and that C—C bond formation occurs in a concerted fashion. This area remains an opportunity for investigation especially as interest in cross coupling with iron and cobalt continues to grow.

Exploring Oxidative Addition with Iron: From Redox-Active Pyridine(diimines) to Catalysts for Hydrogen Isotope Exchange in Pharmaceuticals.

Aryl-substituted pyridine(diimine) iron dinitrogen complexes, (^{R}PDI)Fe(N_2)$_n$ (n = 1,2) are effective precatalysts for a host of transformations including alkene hydrogenation,[35] hydrosilylation,[36] hydroboration,[37] alkene-alkene[38] and alkene-diene cycloaddition[39,40] as well as stoi-chiometric CO_2-ethylene coupling.[41] Despite their exceptional catalytic performance and ability to tune the redox potential of the chelate by nearly 480 mV,[42] these compounds are recalcitrant to promote the oxidative addition of non-polar bonds as σ-complexes of H_2 and silanes have been observed in the ground state.[35a,43] Because of their catalytic activity, H—H or Si—H bond cleavage occurs, but is likely reversible and σ-complexes are favored in the observable intermediates.

During the exploration of the functional group tolerance and substrate scope in pyridine(diimine) iron-catalyzed alkene hydrogenation[44] and intramolecular [2+2] alkene-alkene cycloaddition,[39] cleavage of carbon-oxygen bonds in ethers and esters was identified as a competing catalyst deactivation pathway.[45] Allyl-substituted ethers proved particularly problematic as (^{iPr}PDI)Fe(N_2)$_2$ promoted rapid C—O bond cleavage and generated a near equimolar mixture of the corresponding iron allyl and iron alkoxide (Scheme 5a). The analogous pyridine(diimine) cobalt dinitrogen compound, (^{iPr}PDI)CoN_2,[46] proved slightly less prone to oxidative addition and in certain cases, catalytic [2+2] cycloaddition was achieved.[47] In the case of iron, certain 5-coordinate pyridine(diimine) alkyl complexes are known to undergo radical ejection,[48] supporting allyl radical ejection on the putative (^{iPr}PDI)Fe(η^1-C_3H_5)OEt, that would be trapped by another reduced iron complex to yield the observed mixture. This mode of reactivity – one electron oxidation over two metals – is common among reduced pyridine(diimine) iron and cobalt complexes, especially with alkyl halides.[49,50] This behavior was leveraged in iron chemistry to prepare alkyl complexes containing β-hydrogens enabling study of their electronic structure and chain transfer processes relevant to alkene polymerization catalysis.[51]

In contrast, complexes from more traditional, two-electron-at-one-metal center type reactivity, have been isolated upon addition of vinyl acetate to (^{iPr}PDI)Fe(N_2)$_2$ which yielded the corresponding six-coordinate pyridine(diimine)iron vinyl acetate complex (Scheme 5b).[45]

Suspecting that the redox-activity and the diradical character of the pyridine(diimine) chelate rendered the iron too electron deficient to promote observable H—H or Si—H cleavage in the ground state (Scheme 6a), more electron donating and potentially redox *innocent* pincer type ligands were pursued. Our laboratory postulated that replacement of the

Author Manuscript Author Manuscript Author Manuscript Author Manuscript

imine donors with saturated alkyl phosphines would eliminate the conjugated π-system and significantly raise the barrier to electron transfer to the chelate. The tridentate bis(phosphino)pyridine pincer ^{iPr}PNP (2,6-^{i}Pr$_2$P-methylpyridine) was selected for these studies and, while a dinitrogen complex analogous to (^{iPr}PDI)Fe(N$_2$)$_2$ has eluded preparation, the corresponding iron dihydride dinitrogen complex, *cis*-(^{iPr}PNP)FeH$_2$(N$_2$), was prepared by treatment of the corresponding dihalide precursor with NaBEt$_3$H (Scheme 6b).[52] While not accessed from direct oxidative addition of H$_2$ to Fe(0), the spectroscopic NMR data support significant iron(II) dihydride character and demonstrate that a more electron donating pincer promotes H—H cleavage over reductive coupling to the iron(0) η^2-hydrogen complex. More germane to oxidative addition, treatment of *cis*-(^{iPr}PNP)FeH$_2$(N$_2$) with PhSiH$_3$ generated the corresponding iron silyl complex, *cis*-(^{iPr}PNP)FeH(SiH$_2$Ph)(N$_2$) (Scheme 6c). Although the mechanism of this transformation has not been studied, it is plausible that the reaction proceeds by an Fe(0)–Fe(II) redox cycle involving reductive elimination of H$_2$ from *cis*-(^{iPr}PNP)FeH$_2$(N$_2$) followed by oxidative addition of the Si—H bond of the silane. Exposure of *cis*-(^{iPr}PNP)FeH$_2$(N$_2$) to a hydrogen atmosphere resulted in displacement of the N$_2$ ligand and formation of the corresponding dihydrogen complex, (^{iPr}PNP)FeH$_2$(H$_2$), demonstrating the higher barrier for oxidative addition to Fe(II) than to Fe(0). Nevertheless, all of the hydrogen atoms are in rapid exchange at ambient temperature in solution, consistent with previously reported "*cis*" effect in structures of this type.[53] Since this initial report, Kirchner and coworkers reported non-classical polyhydride complexes with various modifications to the PNP-pincer that exhibit high activity for the head-to-head dimerization and the *Z*-selective hydroboration of terminal alkynes.[54]

Contemporary with our report of the synthesis of (^{iPr}PDI)Fe(N$_2$)$_n$ (n = 1,2),[35a] Danopoulos and coworkers described the synthesis and structural characterization of a related complex, (^{iPr}CNC)Fe(N$_2$)$_2$ (^{iPr}CNC = 2,6-bis[(2,6-diisopropylphenyl)imidazol-2-ylidene]pyridine) where the imine donors were replaced by *N*-heterocyclic carbenes.[55] Subsequent experimental and computational studies[56,57] established that the ^{iPr}CNC ligand was acting as a classic π-acceptor, with no evidence for ligand-centered radicals and, therefore, the iron was best described as a hybrid between low-spin Fe(0) and Fe(II). Such an electronic structure description is expected from an 18-electron, coordinatively saturated bis-dinitrogen compound as ligand-redox activity and, hence, radical character, are more common with four-coordinate compounds.[58] The (^{iPr}CNC)Fe(N$_2$)$_2$ complex promoted the oxidative addition of Si—H bonds of both primary and secondary silanes (Scheme 7a),[59] in contrast to (^{iPr}PDI)Fe(N$_2$)$_2$ which forms a bis(silane) σ-complex (Scheme 6a).[35a] The iron complex reported by Danopoulos also promoted the *ortho*-directed C—H oxidative addition benzaldehyde anilide under UV irradiation (Scheme 7b).

An analog of the Danopoulos complex, (H4-^{iPr}CNC)Fe(N$_2$)$_2$ (H$_4$-^{iPr}CNC = 2,6-(2,6-*i*Pr$_2$-C$_6$H$_3$-4,5-H$_2$-imidazol-2-ylidene)$_2$C$_5$H$_3$N), was prepared by our laboratory, where saturated *N*-heterocyclic carbenes were incorporated in to the pincer. The more commonly used unsaturated carbenes were replaced by the saturated variant as part of structure-reactivity studies in iron-catalyzed alkene hydrogenation.[60] During these investigations, it was discovered that (H$_4$-^{iPr}CNC)Fe(N$_2$)$_2$ promoted the deuteration of C(sp^2)—H bonds of arenes at low pressures of D$_2$ gas with predictable, sterically-determined site-selectivity.[61] This selectivity is orthogonal to state-of-the-art iridium catalysts that engage with functional

Author Manuscript Author Manuscript Author Manuscript Author Manuscript

groups to direct C(sp^2)—H and, ultimately, hydrogen isotope exchange (HIE).[62] As a representative example, the deuteriation of *N,N*-dimethylbenzamide takes place *ortho* to the amide functional group if catalyzed by the Crabtree's catalyst, [(COD)Ir(PCy_3)py]PF_6 (Scheme 8a), while the iron catalyst promotes HIE at the sterically accessible *meta* and *para* positions of the ring (Scheme 8b).

Hydrogen isotope exchange is a relevant catalytic reaction employed in drug discovery and registration. The introduction of deuterium and tritium into drug candidates is important for studies on absorption, distribution, metabolism and excretion (ADME), as well as for the preparation of standards for analytical assays.[63] Direct, late-stage introduction of the hydrogen isotope is preferred over multistep synthesis to minimize handling of potentially radioactive compounds. D_2 and T_2 gases are the preferred sources of D and T respectively, over isotopically enriched water and other protic sources, due to their high isotopic purity and to avoid the autoradiolysis risks associated with tritiated water.[64] The iron dinitrogen complex, (H_4-^{iPr}CNC)Fe(N_2)$_2$, exhibited several attractive features for an HIE catalyst including increased activity at lower pressures of D_2 or T_2 and orthogonal site-selectivity to precious-metal catalysts. A significant concern at the onset of the study was the compatibility of the iron catalyst with functional groups found in drug molecules and with the solvents typically used to dissolve such compounds.

Remarkably, (H_4-^{iPr}CNC)Fe(N_2)$_2$ proved highly efficient for the tritiation of a host of pharmaceuticals (Scheme 9). Many drugs were successfully radiolabeled with 25 mol% of the iron compound in *N*-methyl-2-pyrrolidone (NMP) as solvent and employing sub-atmospheric pressures of T_2 gas. Because of the handling of tritium gas and the value associated with most late-stage pharmaceutical compounds, high catalyst-loadings are typically not a concern in most radiolabeling applications. The iron compound, which is highly sensitive to air and moisture, exhibited compatibility with pharmaceutically relevant functional groups including substituted-arenes, pyridines and five-membered heterocycles.

For ADME studies, specific activities between 15 and 20 Ci/mmol are desired. In general, higher specific activities were observed for the tritiation of drugs with the iron catalyst than with the Crabtree's catalyst although it should be noted that more active, second generation catalysts have been reported by Kerr and others.[65] The higher specific activity found with iron is a result of the catalyst accessing all of the sterically accessible C—H bonds, which are higher in number than those activated by the directed the C—H activation operating for the iridium catalyst. The tritiation of Flumazenil, which does not proceed with Crab-tree's catalyst, illustrates this point as the HIE with iron occurs at the C(sp^2)—H position *ortho* to the fluorine. Lower but detectable incorporation of tritium was also observed on the central C—H bond of the imidazole ring and on the ethyl group, yielding an overall activity of 16.1 C_i/mmol. With MK-6096, a specific activity of 57 Ci/mmol was obtained with the iron catalyst, superior to the value of 16.9 C_i/mmol observed with iridium. The improved performance of the iron catalyst is a result of the functionalization of seven sterically accessible C—H bonds while the iridium catalyst only promoted exchange at the site proximal to the pyrimidine ring. Similar trends were observed in the tritiations of Cinacalcet and Suvorexant (Scheme 9).

Author Manuscript Author Manuscript Author Manuscript Author Manuscript

The discovery of a rare example of a first-row transition metal catalyst for effective HIE in drug molecules prompted exploration of the fundamental organometallic chemistry underlying catalyst performance. One salient question was the role of oxidative addition – both of H_2 (or isotopologue) and the C—H bond – and what role, if any, these fundamental transformations played in the improved activity at lower gas pressure and on-site selectivity. To answer this question, our laboratory conducted studies of the HIE pre-catalyst (H_4-^{iPr}CNC)Fe(N_2)$_2$ with dihydrogen.[66] Immediately upon exposure to H_2 in benzene-d_6, two new iron hydride products were observed by ^{1}H NMR spectroscopy and ultimately characterized by single-crystal X-ray diffraction. At relatively low H_2 pressures (<1 atm), *trans*-(H4-^{iPr}CNC)FeH_2(N_2) was observed, while at increased concentrations of dihydrogen the iron(II) dihydride dihydrogen complex, *trans*-(H_4-^{iPr}CNC)FeH_2(η^2-H_2), was formed (Scheme 10). In benzene-d_6 solution both iron(II) dihydrides underwent H—D exchange with the solvent giving rise to various iron isotopologues and isotopomers that were identified by the large isotopic perturbation of resonance of the hydride signals. When *para*-xylene was used as the solvent, C(sp^2)—H oxidative addition is blocked by the methyl groups and *trans*-(H_4-^{iPr}CNC)FeH_2(η^2-H_2) was obtained as a single product.

The solution behavior of both, *trans*-(H_4-^{iPr}CNC)FeH_2(N_2) and *trans*-(H_4-^{iPr}CNC)FeH_2(η^2-H_2), provides insight into the pathway for HIE in arenes and ultimately drug molecules. As the *trans* hydride arrangement in a six-coordinate geometry is preferred, the position *trans* to the pyridine ligand in the pincer is the coordination site for a neutral ligand, N_2, η^2-H_2 and, presumably, the arene substrate in an η^2-π mode. Following arene coordination, cleavage of the C(sp^2)—H bond proceeds either by either σ-bond metathesis or oxidative addition. This process can be repeated several times, resulting in a mixture of (H_4-^{iPr}CNC)Fe$H_{4-x}D_x$ isotopologues that were ultimately observed by ^{1}H NMR spectroscopy. The increased HIE activity at lower pressures of D_2 or T_2 gas can, therefore, be explained by competition between the arene and D_2 (or T_2) for this coordination site, which suppresses HIE activity at higher pressures of added gas as formation of *trans*-(H_4-^{iPr}CNC)FeH_2(η^2-H_2) is favored.

Understanding pincer ligand design has provided insight and guiding principles for enabling oxidative addition with iron. Among tridentate pincers, relatively electron withdrawing and potentially redox-active pyridine(diimines) favor the formation of η-complexes in the ground state upon reaction with non-polar reagents such as H_2 and silanes. Slightly increasing the electron donation of the pincer by replacement of the imine donors with N-heterocyclic carbenes[56a] resulted in more classical oxidative addition (Fe(0)-Fe(II)) and enabled HIE in pharmaceuticals with distinct site-selectivity. An even more electron-donating bis(phosphine)pyridine pincer also supported iron(II) dihydride and dihydride-dihydrogen structures, but catalytic activity has been thus far lacking, presumably due to reticence to undergo reductive elimination. Balancing the electronics of the pincer is a crucial step in developing new C—H functionalization and other catalytic processes with iron.

A second frontier for oxidative addition with iron is the addition of polar substrates, particularly C—X (X = F, Cl, Br, I) bonds. Not only is the oxidative addition of these bonds scarce, but so are catalysts that tolerate these functionalities. For example, the iron HIE precatalyst, (H_4-^{iPr}CNC)Fe(N_2)$_2$, can be deactivated by the presence of carbon-halogen

Author Manuscript Author Manuscript Author Manuscript Author Manuscript

bonds, especially in substrates where C(sp^2)—H oxidative addition is sluggish. Oxidative addition of C—X bonds is particularly relevant for iron-catalyzed cross coupling[67] yet few well-defined examples have been reported.[68]

Oxidative Addition with Cobalt(I).

Cobalt has emerged as a versatile first-row transition metal with myriad applications in catalysis. Cobalt complexes with redox-active ligands or more classical bidentate phosphines have been found highly active and enantioselective for alkene hydrogenation reactions and, in many cases, cobalt offered advantages over precious metals.[69,70] Remarkably, DFT studies revealed that oxidative addition of dihydrogen is likely not operative with both classes of catalysts, although the computed barriers with phosphine-derived catalysts were energetically reasonable.[71] Hopmann computed that redox-active pyridine(diimines) favored a σ-bond metathesis pathway for H_2 activation.[72] On the other hand, phosphine-supported cobalt(II) precatalysts in directed hydrogenation followed a redox-neutral pathway involving metallacyclic intermediates that also accounted for the stereochemical outcome of the reaction.[73] In contrast, with cobalt(0) bis(phosphine) complexes, C—H oxidative addition of aldehydes has been invoked as a plausible step in the dehydrogenation of methanol,[74] in the intermolecular directed hydroacylation of olefins,[75] as well as in the synthesis of cyclobutanones from dienyl aldehydes,[76] where a Co(0)-Co(II) redox cycle may be operative, although direct evidence is lacking.

In light of these observations and the broader interest in catalytic C—H functionalization chemistry with cobalt,[77] our laboratory sought to prepare complexes that would promote two-electron, precious-metal-like oxidative additions of both polar and non-polar bonds. Previous work from our laboratory,[78] Gibson's and others, demonstrated that pyridine(diimine) cobalt alkyl complexes, (PDI)CoR (R = CH_3, CH_2SiMe_3) are effective precatalysts for alkene hydrogenation,[79] hydroboration,[80] hydrosilylation[81] and dehydrogenative silylation.[82] While many cobalt derivatives have been shown to promote alkene hydrofunctionalization reactions,[83] catalysis relying on two-electron redox processes is by comparison much more underdeveloped, and examples of well-defined oxidative addition reactions, particularly those relevant to catalysis, remain rare. Applying the ligand design successful in iron catalysis, (^{iPr}CNC)$CoCH_3$ was synthesized and shown to be an exceptionally active precatalyst for the hydrogenation of alkenes.[84] The cobalt hydride, (^{iPr}CNC)CoH, was independently synthesized and found to undergo intramolecular migration of the hydride to the 4-position of the pyridine ring of the chelate. This type of reactivity hinted at radical character in the pincer ligand. Both spectroscopic and computational studies on the electronic structure of the cobalt hydride support radical character localized on the pyridine ring of the ^{iPr}CNC chelate. This electronic structure renders the cobalt less electron rich and may rationalize why oxidative addition of H_2 to form a cobalt(III) trihydride was not directly observed. As a result, more electron-donating pincers were targeted with the goal of enabling oxidative addition and observation of Co(III) products.

Contemporaneous with our studies, Milstein and coworkers reported the synthesis of (^{iPr}PNP)$CoCH_3$ and made an intriguing claim that the complex was kinetically unstable to

Author Manuscript Author Manuscript Author Manuscript Author Manuscript

the loss of H-atoms from the methylene linkers of the pincer.[85] Our laboratory had independently prepared the corresponding neosilyl derivative, (^{iPr}PNP)CoCH$_2$SiMe3,[86] which, analogously to the methyl derivative, has a planar geometry around the cobalt center. By contrast, (^{iPr}PNP)CoCl,[87] containing a weaker field chloride ligand, was found to be an S =1 complex, consistent with a distorted tetrahedral geometry at the cobalt, highlighting the flexibility in both geometry and magnetic properties available with 3d metals.

Both cobalt alkyl derivatives, (^{iPr}PNP)CoCH$_3$ and (^{iPr}PNP)CoCH$_2$SiMe$_3$, exhibited a rich two-electron oxidative addition chemistry. Treatment of (^{iPr}PNP)CoCH$_3$ with H$_2$ or HC≡CTol (Tol = toluene) resulted in formation of the corresponding 6-coordinate cobalt(III) products (Scheme 11a).[87] More relevant to C—H functionalization, heating (^{iPr}PNP)CoCH$_3$ in benzene-d_6 to 80 °C produced (^{iPr}PNP)CoC$_6$D$_5$ (Scheme 11b) in low yield due to decomposition of the complex from competing P—C bond cleavage of the chelate. The likely pathway for this transformation involves oxidative addition of a C(sp^2)—D bond of C$_6$D$_6$ to form an intermediate cobalt(III) aryl alkyl deuteride, which undergoes reductive elimination of CH$_3$D to generate the observed Co(I)-phenyl product.

Having observed classical oxidative addition behavior in (^{iPr}PNP)Co^{I}—R complexes, the origin of Milstein's claim of radical chemistry in the pincer and H-atom loss from the CH$_2$-linker[85] was studied in more detail. Our laboratory prepared a family of chloride, methyl, acetylide and hydride complexes containing the P-*tert*-butyl variant of the chelate.[88] The larger phosphine substituents were selected for this study to improve the kinetic stability of the cobalt compounds and slow deleterious P—C bond cleavage.[87] Computational and experimental studies established that the bond dissociation free energies (BDFEs) of the benzylic C—H bonds are correlated to the identity of the X-type ligand. Pure σ-donors, such as hydride and methyl, produced the weakest C—H bonds with BDFEs of 42.7 and 44.6 kcal/mol, below the thermodynamic threshold for H$_2$ formation. This "coordination-induced bond weakening"[89] is a result of the acidity of the methylene linker coupled with the energetically accessible Co(I)-Co(II) redox couple. This type of ligand modification chemistry has not been observed with the rhodium congeners, and complexes such as (^{tBu}PNP)RhCH$_3$[90] and (^{tBu}PNP)RhH[91] are thermally stable. The energetically higher one-electron redox couples strengthen the methylene C—H bonds and make ligand modification by homolytic pathways endergonic.

Since these initial reports, the number of well-defined oxidative addition reactions with Co(I), particularly those relevant to catalysis, have continued to grow. During studies in to the cobalt-catalyzed hydrosilylation of CO$_2$,[92] oxidative addition of the primary silane PhSiH$_3$ to (^{tBu}PNP)CoH was observed yielding (^{tBu}PNP)CoH$_2$(SiH$_2$Ph). By contrast, exposure of (^{tBu}PNP)CoH to 4 atm of H$_2$ resulted in broadening of the cobalt-hydride signal in the ^{1}H NMR spectrum, suggesting an equilibrium between (^{tBu}PNP)CoH and (^{tBu}PNP)CoH$_3$. However, unlike with the isopropyl analog, the Co(III) trihydride was not directly observed or isolated, highlighting the impact of the phosphine substituents on the position of the Co(I)-Co(III) equilibrium. Notably, the distorted S = 1 (^{iPr}PNP)CoX (X = chloride, alkoxide) complexes serve as precatalysts for the cross-coupling of aryl triflates with selected furanyl-derived neutral boronic esters.[93] While C—O oxidative addition of the electrophile seems plausible, direct observation of this step has been elusive, and the mode

Author Manuscript Author Manuscript Author Manuscript Author Manuscript

of substrate activation and the fundamental reasons for successful cross coupling have not been fully established. Not only neutral cobalt(I) ^{iPr}PNP complexes are able to promote oxidative addition, but also the cationic cobalt(I) dinitrogen complex, [(^{iPr}PNP)Co(N_2)]BArF^{24} (BArF^{24}= B[C_6H_3–3,5-(CF_3)$_2$]$_4$), which has been recently found to reversibly cleave H_2 yielding the cationic cobalt(III) derivative [(^{iPr}PNP)CoH_2(N_2)] BArF^{24}.[94]

Fout and coworkers have developed the chemistry of cobalt(I) precursors bearing tridentate, monoanionic aryl-bis(carbene) pincers (Scheme 12),[95] where a host of oxidative addition and catalytic chemistry has been observed. For example, exposure of (^{Mes}CCC)CoN_2(PPh_3) (^{Mes}CCC = bis(mesityl-benzimidazol-2-ylidene)phenyl) to a mixure of H_2 and D_2 resulted in isotopic exchange forming H—D and the non-classical cobalt hydrogen-deuterium complex (^{Mes}CCC)Co(HD)(PPh_3) (Scheme 12a). Formation of free H—D is proposed to occur through an oxidative addition-reductive elimination sequence, similar to that observed with the isoelectronic (H_4-^{iPr}CNC)Fe(N_2)$_2$.[66] Further demonstration of the oxidative addition reactivity of the (^{Mes}-CCC)CoN_2(PR_3) (R = Ch_3, Ph) family of complexes was demonstrated by addition of HCl to the PMe_3 derivative to form the cobalt(III) product, (^{Mes}CCC)CoH(Cl) (PMe_3) (Scheme 12a). In addition, (^{Mes}CCC)CoN_2(PPh_3) has been found to be an efficient precatalyst for alkene hydrogenation and para-hydrogen induced polarization (PHIP) NMR experiments support oxidative addition of H_2 to form Co(III) (Scheme 12b). These complexes are also active for alkene hydrosilylation and hydroboration and are proposed to operate by a Co(I)-Co(III) cycle featuring an H—Si and H—B oxidative addition respectively.[96]

Cobalt-Catalyzed C(sp²)—H Borylation.

Metal-catalyzed C(sp^2)—H borylation has emerged as a powerful and widely adopted C—H functionalization method owing to the versatility of the carbon-boron bond[97] and predictable site-selectivity of the catalytic reaction.[98,99] State-of-the-art catalysts rely on iridium(I) precursors in combination with bidentate phosphine or, more commonly, bipyridine ligands, and operate by an accepted Ir(III)-Ir(V) cycle involving rate-determining oxidative addition of the C(sp^2)—H bond to an Ir(III) tris(boryl) intermediate.[100] The successful C(sp^2)—H activation of benzene by (^{iPr}PNP)CoCH_3 suggested that a related Co(I) boryl may be active for catalytic borylation chemistry. Preparation of a putative (^{iPr}PNP)CoBPin would also provide insight as to how many boryl ligands (the active Ir catalyst has three) are required for effective turnover.

Initial studies featured (^{iPr}PNP)CoCH_2SiMe_3 as the precatalyst for the C(sp^2)—H borylation of arenes, pyridines and 5-memberring heterocycles using either HBPin or B_2Pin_2 as the boron source.[86] With 5-membered heterocycles such as methyl furan 2-carboxylate, up to 5000 turnovers were observed with HBPin and only 0.2 mol% of cobalt precatalyst (Scheme 13), and the most acidic position, typically the 5-position of the heterocycle, was the site of C—H functionalization. With arenes and pyridines, B_2Pin_2 was used as the boron source and, in most cases (see below), the selectivity of the reaction was governed, much like iridium, by the steric accessibility of the C(sp^2)—H bond. For example, with 2,6-lutidine, borylation was observed exclusively at the 4-position of the ring (Scheme 13b), while with

Author Manuscript Author Manuscript Author Manuscript Author Manuscript

2,4-lutidine and 2-methoxy-4-methylpyridine, C—B bond formation occurred exclusively in the 2-position. The latter substrates are noteworthy as they are challenging substrates for iridium, demonstrating that first-row metal catalysts, have the potential to offer unique reactivity.

Mechanistic insights into cobalt-catalyzed C(sp^2)—H borylation: Arenes and pyridines.

The observation of efficient C(sp^2)—H borylation with a well-defined cobalt(I) alkyl precatalyst raised questions as to the mechanism of the reaction, including the identity of the C—H activating species and the cobalt oxidation states accessed during turnover. Monitoring the borylation of 2,6-lutidine by ^{1}H and ^{31}P NMR spectroscopy established two resting-states for the cobalt catalyst – one at low conversion of substrate and a second that appears during the latter stages of the reaction.[101] The spectroscopic data for both compounds unequivocally established borylation of 4-position of the pincer. Moreover, borylation of the cobalt complex competes with that of the 2,6-lutidine and occurs previous to turnover. As a result, the resting-state at early conversion was identified as the cobalt(I) boryl complex, (4-BPin-^{iPr}PNP)Co(BPin)(N_2), while the latter stage compound was the corresponding Co(III) derivative, *trans*-(4-BPin-^{iPr}PNP)CoH_2(BPin).

One immediate question was how chelate borylation impacted reactivity and the overall performance of the catalyst. To address this issue, identification of the compound responsible for C—H activation and the overall turnover-limiting step in the process were critical. Addition of one equivalent of B_2Pin_2 to (^{iPr}PNP)CoCH_2SiMe_3 generated the cobalt(I) boryl, (^{iPr}PNP)Co(BPin)(N_2) where the pyridine ring remains intact (Scheme 14a). This complex was unstable to vacuum, likely due to N_2 dissociation, however, the related carbonyl derivative, (^{iPr}PNP)Co(BPin)(CO) (Scheme 14a), was vacuum-stable and could be isolated and characterized by single crystal X-ray diffraction. In contrast, when excess B_2Pin_2 was added to (^{iPr}PNP)CoCH_2SiMe_3, borylation of the pyridine ring of the pincer occurred, yielding (4-BPin-^{iPr}PNP)Co(BPin)(N_2) (Scheme 14b), supporting borylation of the ligand during catalytic turnover. Both stoichiometric experiments identified (4-BPin-^{iPr}PNP)Co(BPin) as the C—H activating species. Further reaction of (4-BPin-^{iPr}PNP)Co(BPin)(N_2) with excess HBPin afforded *trans*-(4-BPin-^{iPr}PNP)CoH_2(BPin) (Scheme 14b), hinting that the second resting-state in borylation is formed as a result of increasing HBPin concentration during turnover.

The rate law for the cobalt-catalyzed borylation of 2,6-lutidine was established as first order with respect to both the cobalt precursor and the pyridine substrate. This observation, in combination with an observed primary deuterium kinetic isotope effect of 2.9(1) at 80 °C (for the borylation of 2,6-lutidine versus 4-d-2,6-lutidine, measured in separate vessels), supports the mechanism proposed in Scheme 15. The cobalt(I) alkyl enters the catalytic cycle by reaction with B_2Pin_2 to form (4-BPin-^{iPr}PNP)Co(BPin). This compound promotes the oxidative addition of the C(4)—H bond of 2,6-lutidine to generate a 6-coordinate cobalt(III) lutidinyl boryl hydride, which undergoes C—B reductive elimination to generate the aryl boronate product and the cobalt (I) hydride (4-BPin-^{iPr}PNP)CoH. Regeneration of

Author Manuscript Author Manuscript Author Manuscript Author Manuscript

the cobalt(I) boryl occurs by oxidative addition of B_2Pin_2 to the cobalt hydride followed by reductive elimination of HBPin. The cobalt(I) hydride also reacts with the HBPin that accumulates in the reaction medium at high substrate conversion, yielding the observed resting state *trans*-(4-BPin-^{iPr}PNP)CoH_2(BPin).

Because oxidative addition of the C(sp^2)—H bond is turnover limiting, the electronic effect of the boron substituent on the electron-donating and -releasing properties of the pincer was examined. Electrochemical measurements established the 4-boryl substituted pincer as *less* electron donating than the parent ^{iPr}PNP, in turn slowing oxidative addition. To prevent PNP borylation, second-generation cobalt precatalysts of the type (4-R-^{iPr}PNP)CoH_2(BPin) [R = Me, pyrr (pyrr = pyrrolidinyl)] were synthesized and evaluated for the catalytic borylation of pyridines and arenes. The 4-substituents serve the dual purpose of preventing borylation of the pyridine and making the pincer more electron-rich, therefore increasing the rate of turnover-limiting C(sp^2)—H oxidative addition (Scheme 16a).

Second-generation catalysts exhibited improved performance in the borylation of 2,6-lutidine with B_2Pin_2. The cobalt compound bearing the most electron donating pincer, (4-pyrr-^{iPr}PNP)CoH_2(BPin), produced the highest turnover frequencies. While mechanistic studies, again, support a Co(I)-Co(III) cycle, the deuterium kinetic isotope effect (k_H/k_D = 1.6(1) at 80 °C) supports a transition in the rate-determining step from oxidative addition to reductive elimination. This shift in the rate-determining step is likely a result of the overall electron density at cobalt, where a more donating pincer favors the oxidation of cobalt (I) by stabilization of the cobalt (III) complexes, leading to a more kinetically challenging C—B reductive elimination (Scheme 16b).

With firm support for the pathway of catalytic borylation of lutidine with B_2Pin_2, additional studies were conducted to explore the role of the HBPin byproduct and why this boron reagent was ineffective for the functionalization of pyridines and arenes. Monitoring the borylation of 2,6-lutidine with HBPin in the presence of catalytic (^{iPr}PNP)$CoCH_2SiMe_3$ revealed the formation of (4-BPin-^{iPr}PNP)Co(H)(PH^iPr_2), arising from P—C bond cleavage of the pincer along with other unidentified cobalt products.[102] The product from P—C bond cleavage, (4-BPin-^{iPr}PNP)Co(H)(PH^iPr_2), was inactive for borylation and likely forms as a result of competitive HBPin reductive elimination from (4-BPin-^{iPr}PNP)CoH_2(BPin) (instead of H_2). This would yield metastable (4-BPin-^{iPr}PNP)CoH, which undergoes P—C bond cleavage, as previously reported for (^{iPr}PNP)CoH.[87]

A detailed computational analysis of the mechanism of the cobalt catalyzed C(sp^2)—H borylation of benzene was conducted by Hall and coworkers.[103] The overall energetically preferred pathway was consistent with the mechanism proposed in Scheme 15. A key finding of these studies was the importance of PNP conformational dynamics in fundamental transformations such as oxidative addition and reductive coupling and ultimately elimination. Alternative pathways involving σ-bond metathesis for C—H oxidative addition, and phosphine dissociation for reductive elimination, were ruled out as less accessible routes. The results also revealed that the preferred trajectory for benzene C(sp^2)—H oxidative addition was parallel to the P—Co—P axis.

Author Manuscript Author Manuscript Author Manuscript Author Manuscript

Studies in to the Mechanism of Cobalt-Catalyzed Heteroarene Borylation with HBPin.

The discovery of the deleterious effect of HBPin on the borylation of 2,6-lutidine, raised the question as to why this boron reagent was effective for reactions with 5-membered heterocycles. A combination of deuterium kinetic isotope effect measurements, rate-law determination and stoichiometric reactions was conducted with 2-methylfuran and (^{iPr}PNP)CoCH$_2$SiMe$_3$ as the precatalyst.[102] The cobalt(III) dihydride boryl, *trans*-(^{iPr}PNP)CoH$_2$(BPin) was identified as the resting-state at both high and low substrate conversion. The overall first order rate law (rate = *kobs*[Co]^1[substrate]^0[HBPin]^0) suggested that the reductive elimination of H_2 rather than the C—H oxidative addition is the turnover limiting step in the catalytic cycle (Scheme 17).

The second generation precatalyst, (4-pyrr-^{iPr}PNP)CoCH$_2$SiMe$_3$, bearing an electron donating pyrrolidinyl group in the 4-position of the pincer, was *less active* for the borylation reaction, whereas, (4-BPin-^{iPr}PNP)CoCH$_3$, containing an electron-withdrawing group, was *more active*. Both results are consistent with reductive elimination as the turnover limiting step and highlight not only the relevance of mechanistic studies to improve catalyst design, but also that catalyst optimization can be highly dependent on the class of substrates.

C(sp^2)—H Borylation of Fluorinated Arenes: Highly Ortho-to-fluorine Site-Selective Cobalt Catalysts.

While pincer-supported cobalt catalysts operate in a similar manner to precious metal catalysts involving oxidative addition of a C(sp^2)—H bond to a metal-boryl followed by C—B reductive elimination, the first-row metal offers the opportunity to discover reactivity distinct from iridium. Both the well-defined (4-Me-^{iPr}PNP)Co(BPin)H$_2$, and the bench-stable (4-Me-^{iPr}PNP)Co(O$_2$CtBu)$_2$ precatalysts, offer unique and synthetically useful *ortho* to fluorine selectivity for the borylation of fluorinated arenes (Scheme 18).[104] Given the prevalence of fluorinated arenes in pharmaceuticals[105] and agrochemicals,[106] methods for their selective functionalization are valuable in synthesis.

Remarkably, the cobalt catalysts retain their preference for *ortho*-to-fluorine site-selectivity even in the presence of directing groups, likely arising from the coordinative saturation of the (4-Me-^{iPr}PNP)CoH(^{F}Ar)(BPin) intermediate which prevents additional coordination of directing groups (Scheme 19). Thus, cobalt C(sp^2)—H borylation catalysts, much like iron catalysts for HIE, ignore directing groups and offer complementary products to those obtained from iridium catalysis. From a more fundamental point of view, these results demonstrate the utility of substitutional lability and help to rationalize the role of coordinative saturation in achieving unique site-selectivity.

The air-stable cobalt(II) bis(carboxylate) precatalyst, (4-Me-^{iPr}PNP)Co(O$_2$C*t*Bu)$_2$ is prepared in a straightforward manner from addition of the free pincer to Co(O$_2$CtBu)$_2$ and is a high spin, $S = 3/2$ compound. Metal carboxylates have proven to be an effective strategy for generating air-stable precursors with first-row transition metals, particularly cobalt and nickel.[81,107,108,109] This strategy is underdeveloped with iron and represents an important

Author Manuscript Author Manuscript Author Manuscript Author Manuscript

area for future research. Importantly, upon activation with HBPin, (4-Me-^{iPr}PNP)Co(O_2CtBu)$_2$ exhibited comparable activity and site-selectivity to the well-defined cobalt(III) complex, (4-Me-^{iPr}PNP)CoH_2(BPin). However, the cobalt(II) bis(carboxylate) precatalyst exhibited an induction period on the order of 12 hours arising from the time required to convert the carboxylate ligands to the active cobalt(I) boryl.[110] Formation of the catalytically inactive Co{PinB(O_2CtBu)$_2$}$_2$ complex accompanies generation of the active species.[111]

Beyond PNP Ligands: Cobalt-Catalyzed Borylation with Other Tridentate Pincers.

Since the discovery and report of catalytic borylation with [(^{iPr}PNP)Co]-derived catalysts, a variety of other neutral, tridentate pincer ligands have been evaluated (Scheme 20).[112] Fundamental organometallic chemistry motivated these studies with the open question as to what are the electronic and steric properties of supporting ligands to generate a cobalt(I) boryl that will promote oxidative addition of C(sp^2)—H bonds. As presented in Scheme 20, a variety of nitrogen- and phosphorus-containing pincers were evaluated. In general, most of these complexes exhibit inferior activity to as compared to [(^{iPr}PNP)Co].

The phosphine-substituted bipyridine pincer, ^{iPr}PBipy (6-diisopropylphosphinomethyl-2,2'-bipyridine) and the related and less expensive neocuproine derivative, ^{iPr}PNeo (2-diisopropylphosphinomethyl-9-methyl-1,10-phenanthroline) were explored as hybrid electron-donating yet potentially redox-active ligands. Previous studies had also demonstrated that in-situ activation of the cobalt dichloride, (^{iPr}PBipy)CoCl_2 with Na-BEt_3H produced an active catalyst for alkene hydroboration.[113] Cobalt(I) methyl complexes, (^{iPr}PBipy)CoCH_3 and (^{iPr}PNeo)CoCH_3 were synthesized in an attempt to gain insight in to the poor C(sp^2)—H borylation performance. Addition of excess HBPin to (^{iPr}PBipy)CoCH_3 generated a mixture of products, one of which was the expected Co(III) dihydride boryl, *trans*-(^{iPr}PBipy)CoH_2(BPin). This compound undergoes facile reductive elimination and is in equilibrium with the Co(I) hydride, (^{iPr}PBipy)CoH, which was not directly observed but inferred from NOESY spectroscopy and by trapping with 3,3-dimethylbutene. in the absence of HBPin, a paramagnetic product identified as the mixed-valent cobalt hydride, [(^{iPr}PBipy)Co]$_2$(μ_2-H), was formed, which is inactive for borylation (Scheme 21). The tendency of the (^{iPr}PBipy)CoH complex to undergo H_2 loss is attributed to the weakly electron donating nature of the pincer which disfavors oxidative addition, making other pathways more kinetically viable. Moreover, redox-activity of the pincer was also pointed as detrimental for catalytic activity as this behavior generally reduces the electronic density at the metal.

One often cited motivation for catalysis with Earth-abundant metals is catalyst cost. in many cases, the cost of preparing the ligand far exceeds the cost of even a precious metal. An emphasis in our research group has been on the use of readily prepared, inexpensive and air-stable ligands. 4-Substituted terpyridines were attractive due to their air-stability as well as their straightforward and scalable syntheses (Scheme 22a)[114] and lack of P—C bonds for rupture and catalyst deactivation. The corresponding cobalt(II) bis(acetate) derivative,

Author Manuscript Author Manuscript Author Manuscript Author Manuscript

(^{Ar}terpy)Co(OAc)$_2$ (Ar = 4-dimethylaminophenyl, terpy = 2,2':6',2"-terpyridine) was prepared and shown to promote the C(sp^2)—H borylation of selected arenes and heteroarenes (Scheme 22b and c).[111] While the scope and performance of (^{Ar}terpy)Co(OAc)$_2$ was inferior to the [(^{iPr}PNP)Co] family of precatalysts, the straightforward access to the former makes it attractive if a sufficiently activated C(sp^2)—H bond is present. Bis(chelate) cobalt complexes were identified as deactivation products, highlighting the advantage of steric protection for catalyst fidelity.

Cui, Driess and coworkers have reported the synthesis of a cobalt(II) dibromide complex with a tridentate pyridine bis(silylene) pincer, (SiNSi)CoBr$_2$ (SiNSi = 2,6-[EtNSi(NtBu)$_2$CPh]$_2$C$_5$H$_3$N). Upon addition of two equivalents of NaBEt$_3$H and a stoichiometric quantity of cyclohexene, C(sp^2)—H borylation of furans, pyridines and several fluorinated arenes was observed (Scheme 23).[115] A notable feature of this catalyst is the *meta* to fluorine site-selectivity, complementary to the (^{iPr}PNP)CoCH$_2$SiMe$_3$ precatalyst. However, the lack of identification of the active species, the cobalt redox cycle and the role of the cyclohexene additive prevent understanding the origin of this reversal in selectivity. These studies nevertheless demonstrate the potential of first-row transition metals in selective C—H functionalization chemistry.

Our laboratory has also explored replacing the electron-donating, redox-innocent tridentate pincers with redox-active bidentate μ-diimines. The cobalt(II) dialkyl, (^{iPr}DI)Co(CH$_2$SiMe$_3$)$_2$ (^{iPr}DI = [2,6-^{i}Pr$_2$C$_6$H$_3$N=C(CH$_3$)]2) and the air-stable Co(^{Cy}ADI)(O$_2$CR)$_2$ (^{Cy}ADI = C$_6$H$_{11}$N=C(CH$_3$)]$_2$, R = 3-heptyl), catalyze the H—D exchange (Scheme 24a)[116] and the borylation (Scheme 24b),[117] respectively, of C(sp^3)—H bonds in the presence of C(sp^2)—H bonds. The paramagnetism and high reactivity of these complexes has thus far complicated mechanistic study and additional efforts are needed to explore the active species and the origin of the unique site-selectivity. Following this discovery, Smith, Maleczka, Oppenheim and coworkers reported cobalt(II) bis(*tert*-butoxide) NHC complexes that promote benzylic borylation of alkyl arenes with HBPin.[118]

Conclusions and Outlook.

Motivation for catalysis with relatively Earth-abundant, first-row transition metals include potential for improved catalyst cost, toxicity and environmental foot-print. Just as enticing however, is the possibility for new chemistry, distinct from precious metals, arising from unique electronic structures or coordination environments. Central to this opportunity, is the study and, ultimately, the development of fundamental organometallic chemistry.

The redox- and geometric-flexibility of iron and cobalt raises the question as to what redox couple(s) are optimal for oxidative addition and reductive elimination sequences in various catalytic transformations. The variability in redox states may present a challenge initially but, once understandings of ligand design and coordination chemistry, this flexibility may be leveraged to open new reactivity channels.

While oxidative addition to iron(0) has been known for decades, until recently this chemistry was limited to stoichiometric examples. Through creative ligand design and applications of

Author Manuscript Author Manuscript Author Manuscript Author Manuscript

photochemistry, catalytic processes such as hydrogen isotope exchange in pharmaceuticals and C—H borylation chemistry have been realized. Cobalt has followed a similar trajectory with rare examples of stoichiometric oxidative addition chemistry that, over time, evolved in to examples of catalytic reactions that involve two-electron bond-breaking processes as a key substrate activation step.

With both iron and cobalt, catalytic C—H functionalization offers considerable promise that extends beyond the traditional motivations for catalysis with Earth-abundant elements. In both, hydrogen isotope exchange chemistry and C—H borylation, directing groups, commonly used in precious-metal catalysis to bias site-selectivity, are ignored by the first-row metal offering complementary reactivity. In addition, cobalt-catalyzed borylation offers unique “electronically-enhanced” site-selectivity with fluorinated arenes. Future studies are needed to uncover the origin of this behavior and whether this extends to functional groups beyond fluorine. The ability to selectively functionalize C(sp^2)—H bonds based on subtle electronic differences rather than steric effects or directing groups will be transformative in organic synthesis. Clearly, the future of iron and cobalt in C—H functionalization catalysis is a promising one.

Despite these successes, catalysis with iron and cobalt remains in its infancy and many challenges, both fundamental and applied, remain. With high-throughput experimentation, now a widely deployed method of catalyst discovery and optimization,[119] versatile iron and cobalt precursors are needed that form precatalysts with an array of ligand types. Air- and water-stable precursors and precatalysts are often essential, especially in cases where “drop-in” precious-metal replacement technology is desired. A related challenge is functional-group tolerance where state-of-the-art iron and cobalt catalysts are often more sensitive than many precious metal catalysts. These latter two properties are some of the most difficult to optimize in molecular catalysis.

Oxidative addition of relatively non-polar bonds such as H-H, Si-H, C—H, B-H and B-B is now well-established with iron and cobalt and a host of catalytic reactions, in some cases with superior activity and novel selectivity to precious-metals, have been discovered. A frontier for these metals is the oxidative addition of polar bonds such as carbon-halogen and carbon-oxygen.[120] Efforts in this area are sorely needed and, once understood, this knowledge can be applied to cross coupling and other important processes involving substrates of this type. As with the non-polar reagents presented here, the interplay of fundamental organometallic reaction chemistry with new applications will facilitate discovery.

ACKNOWLEDGMENTS

R.A. acknowledges the Principado de Asturias-FICYT and the European Union for a Marie Curie Clarín-COFUND fellowship. P. J. C. acknowledges initial financial support from the Packard Foundation to develop fundamental chemistry for catalysis with Earth abundant elements. Current financial support from the National Institutes of Health (5R01GM121441) is gratefully acknowledged. P. J. C. also thanks the dedicated graduate students, postdoctoral researchers, visiting scientists and industrial collaborators for their contributions in developing catalysis with iron and cobalt.

Author Manuscript Author Manuscript Author Manuscript Author Manuscript

REFERENCES

1. Labinger JA Tutorial on oxidative addition Organometallics 2015, 34, 4784–4795.
2. Li J; Albrecht J; Borovika A; Eastgate MD Evolving green chemistry metrics into predictive tools for decision making and bench-marking analytics. ACS Sustainable Chem. Eng 2018, 6, 1121–1132.
3. Poliakoff M; Licence P; George MW A new approach to sustainability: A Moore's law for chemistry. Angew. Chem. Int. Ed 2018, 57, 12590–12591.
4. Egorova KS; Ananikov VP Which metals are green for catalysis? Comparison of the toxicities of Ni, Cu, Fe, Pd, Pt, Rh and Au salts. Angew. Chem. Int. Ed 2016, 55, 12150–12162.
5 (a). Bauer I; Knölker H-J Iron Catalysis in Organic Synthesis. Chem. Rev 2015, 115, 3170–3387. [PubMed: 25751710] (b)Fürstner A Iron Catalysis in Organic Synthesis: A Critical Assessment of What It Takes To Make This Base Metal a Multitasking Champion. ACS Cent. Sci 2016, 2, 778–789. [PubMed: 27981231] (c)Ludwig JR; Schindler CS Catalyst: Sustainable Catalysis. Chem 2017, 2, 313–316.(d)Piontek A; Bisz E Szostak M iron-catalyzed cross-coupling in the synthesis of pharmaceuticals: In pursuit of sustainability. Angew. Chem. Int. Ed 2018, 57, 11116–11128.(e)Hayler JD; Leahy DK; Simmons EM A pharmaceutical perspective on sustainable metal catalysis. Organometallics 2019, 38, 36–46.
6 (a). Holland PL Distinctive reaction pathways at base metals in high-spin organometallic catalysts Acc. Chem. Res 2015, 48, 1696–1702. [PubMed: 25989357] (b)Zell TZ; Langer R From ruthenium to iron and manganese – A mechanistic view on challenges and design principles of base-metal hydrogenation catalysts. ChemCatChem 2017, 10, 1930–1940.
7. Darmon JM; Stieber SCE; Sylvester KT; Fernandez I; Lobkovsky E; Semproni SP; Bill E; Wieghardt K; DeBeer S; Chirik PJ Oxidative addition of carbon-carbon bonds with a redox-active bis(imino)pyridine iron complex. J. Am. Chem. Soc 2012, 134, 17125–17137. [PubMed: 23043331]
8 (a). Jacquet J; Desage-El Murr M; Fensterbank L Metal-promoted coupling reactions implying ligand-based redox changes. ChemCatChem 2016, 8, 3310–3316.(b)Broere DLJ; Plessius R; van der Vlugt JI New avenues for ligand-mediated processes – expanding metal reactivity by the use of redox-active catechol, o-aminophenol and o-phenylenediamine ligands. Chem. Soc. Rev 2015, 44, 6886–6915. [PubMed: 26148803] (c)Luca OR; Crabtree RH Redox-active ligands in catalysis Chem. Soc. Rev 2013, 42, 1440–1459. [PubMed: 22975722]
9 (a). Oren D; Diskin-Posner Y; Avrarn L; Feller M; Milstein D Metal-ligand cooperation as key in formation of dearomatized Ni(II)-H pincer complexes and in their reactivity toward CO and CO_2. Organometallics 2018, 37, 2217–2221. [PubMed: 31080304] (b)Karunananda M; Mankad NP Cooperative strategies for catalytic hydrogenation of unsaturated hydrocarbons. ACS Catal. 2017, 7, 6110–6119.(c)Zell T; Milstein D Hydrogenation and dehydrogenation iron pincer catalysts capable of metal-ligand cooperation by aromatization/dearomatization. Acc. Chem. Res 2015, 48, 1979–1994. [PubMed: 26079678] (d)Gunanathan C; Milstein D Metal-ligand cooperation by aromatization-dearomatization: A new paradigm in bond activation and "green" catalysis. Acc. Chem. Res 2011, 44, 588–602. [PubMed: 21739968]
10 (a). Mazzacano TJ; Mankad NP Base Metal Catalysts for Photochemical C—H Borylation That Utilize Metal–Metal Cooperativity. J. Am. Chem. Soc 2013, 135, 17258–17261. [PubMed: 24074248] (b)Parmelee SR; Mazzacano TJ; Zhu Y; Mankad NP; Keith JA A Heterobimetallic Mechanism for C—H Borylation Elucidated From Experimental and Computational Data. ACS Catalysis 2015, 5, 3689–3699.(c)Mankad NP Non-Precious Metal Catalysts for C—H Borylation Enabled by Metal–Metal Cooperativity. Synlett 2014, 25, 1197–1201.
11. Lopez KG; Cundari TR; Gary JB Cooperative metal plus ligand oxidative addition and sigma-bond metathesis: A DFT study. Organometallics 2018, 37, 309–313.
12. Krautwald S; Bezdek MJ; Chirik PJ Cobalt-catalyzed 1,1-diboration of terminal alkynes: Scope, mechanism, and synthetic applications. J. Am. Chem. Soc 2017, 139, 3868–3875. [PubMed: 28199104]
13. Hata G; Kondo H; Miyake A Ethylenebis(Diphenylphosphine) Complexes of Iron and Cobalt. Hydrogen Transfer Between the Ligand and Iron Atom. J. Am. Chem. Soc 1968, 90, 2278–2281.
14. Jonwicz AH; Bergman RG C—H activation in completely saturated hydrocarbons – Direct observation of M + R—H M(R)(H). J. Am. Chem. Soc 1982, 104, 352–354.

Author Manuscript Author Manuscript Author Manuscript Author Manuscript

15. Hoyano JK; Graham WAH Oxidative addition of the carbon-hydrogen bonds of neopentane and cyclohexane to a photochemically generated iridium(I) complex. J. Am. Chem. Soc 1982, 104, 3723–3275.

16. Ittel SD; Tolman CA; Krusic PJ; English AD; Jesson JP Bis(Diphenylphosphino)ethane complexes of iron. Inorg. Chem 1978, 17, 3432–3438.

17. Azizian H; Morris RH Photochemical Synthesis and Reactions of $FeH(C_6H_4PPhCH_2CH_2PPh_2)$ $(PPh_2PCH_2CH_2PPh_2)$. Inorg. Chem 1983, 22, 6–9.

18 (a). Tolman CA; Ittel SD; English AD; Jesson JP The Chemistry of 2-Naphthyl Bis[Bis(Dimethylphosphino)Ethane] Hydride Complexes of Iron, Ruthenium, and Osmium. 1. Characterization and Reactions with Hydrogen and Lewis Base Ligands. J. Am. Chem. Soc 1978, 100, 4080–4089.(b)Ittel SD; Tolman CA; English AD; Jesson JP The Chemistry of 2-Naphthyl Bis[Bis(Dimethylphosphino)Ethane] Hydride Complexes of Iron, Ruthenium, and Osmium. 2. Cleavage of sp and sp^3 Carbon-Hydrogen, Carbon-Oxygen, and Carbon-Halogen Bonds. Coupling of Carbon Dioxide and Acetonitrile. J. Am. Chem. Soc 1978, 100, 7577–7585. (c)Tolman CA; Ittel SD; English AD; Jesson JP Chemistry of 2-Naphthyl Bis[Bis(Dimethylphosphino)Ethane] Hydride Complexes of Iron, Ruthenium, and Osmium. 3. Cleavage of sp^2 Carbon-Hydrogen Bonds. J. Am. Chem. Soc 1979, 101, 1742–1751.

19 (a). Field LD; George AV; Messerle BA Methane Activation by an Iron Phosphine Complex in Liquid Xenon Solution. J. Chem. Soc., Chem. Commun 1991, 19, 1339–1341.(b)Baker MV; Field LD Reaction of sp^2 Carbon-Hydrogen Bonds in Unactivated Alkenes with Bis(Diphosphine) Complexes of Iron. J. Am. Chem. Soc 1986, 108, 7433–7434.(c)Baker MV; Field LD Reaction of Carbon-Hydrogen Bonds in Alkanes with Bis(Diphosphine) Complexes of Iron. J. Am. Chem. Soc 1987, 109, 2825–2826.

20. Dombray T; Werncke CG; Jiang S; Grellier M; Vendier L; Bontemps S; Sortais J-B; Sabo-Etienne S; Darcel C Iron-Catalyzed C—H Borylation of Arenes. J. Am. Chem. Soc 2015, 137, 4062–4065. [PubMed: 25782140]

21 (a). Waltz KM; He X; Muhoro C; Hartwig JF Hydrocarbon Functionalization by Transition Metal Boryls. J. Am. Chem. Soc 1995, 117, 11357–11358.(b)Waltz KM; Hartwig JF Selective Functionalization of Alkanes by Transition-Metal Boryl Complexes. Science 1997, 277, 211–213.(c)Waltz KM; Muhoro CN; Hartwig JF C—H Activation and Functionalization of Unsaturated Hydrocarbons by Transition-Metal Boryl Complexes. Organometallics 1999, 18, 3383–3393.(d)Waltz KM; Hartwig JF Functionalization of Alkanes by Isolated Transition Metal Boryl Complexes. J. Am. Chem. Soc 2000, 122, 11358–11369.(e)Taylor KH; Kalman SE; Gunnoe TB; Sabat M Combined Furan C—H Activation and Furyl Ring-Opening by an Iron(II) Complex. Organometallics 2016, 35, 1978–1985.(f)Mazzacano TJ; Mankad NP Thermal C—H Borylation Using a CO-Free Iron Boryl Complex. Chem. Commun 2015, 51, 5379–5382.(g)Ohki Y; Hatanaka T; Tatsumi K C—H Bond Activation of Heteroarenes Mediated by a Half-Sandwich Iron Complex of N-Heterocyclic Carbene. J. Am. Chem. Soc 2008, 130, 17174–17186. [PubMed: 19007215] (h)Kalman SE; Petit A; Gunnoe TB; Ess DH; Cundari TR; Sabat M Facile and Regioselective C—H Bond Activation of Aromatic Substrates by an Fe(II) Complex Involving a Spin-Forbidden Pathway. Organometallics 2013, 32, 1797–1806.

22. Hatanaka T; Ohki Y; Tatsumi K C—H Bond Activation/Borylation of Furans and Thiophenes Catalyzed by a Half-Sandwich Iron N-Heterocyclic Carbene Complex. Chemistry – An Asian Journal 2010, 5, 1657–1666.

23. Webster CE; Fan Y; Hall MB; Kunz D; Hartwig JF Experimental and Computational Evidence for a Boron-Assisted, σ-Bond Metathesis Pathway for Alkane Borylation. J. Am. Chem. Soc 2003, 125, 858–859. [PubMed: 12537470]

24. Jones WD; Foster GP; Putinas JM The Catalytic Activation and Functionalization of Carbon-Hydrogen Bonds. Aldimine Formation by the Insertion of Isonitriles Into Aromatic Carbon-Hydrogen Bonds. J. Am. Chem. Soc 1987, 109, 5047–5048.

25. Ringenberg MR; Gray DL; Rauchfuss TB Oxidative addition of a diphosphine anhydride to iron(0) and nickel(0): A simple approach to installing four ligands. Organometallics 2011, 30, 2885–2888.

26. Casitas A; Krause H; Lutz S; Goddard R; Bill E; Furstner A Ligand Exchange on and Allylic C—H Activation by Iron(0) Fragments: π-Complexes, Allyliron Species, and Metallacycles. Organometallics 2018, 37, 5, 729–739.

Author Manuscript Author Manuscript Author Manuscript Author Manuscript

27. Basallote MG; Hughes DL; Jiménez-Tenorio M; Leigh GJ; Vizcaíno MCP; Jiménez PV Chemistry of Cobalt Complexes with 1,2-Bis-(Diethylphosphino)Ethane: Hydrides, Carbon Disulfide Complexes, and C—H Cleavage in Activated Alk-1-ynes. Crystal Structure of [CoH(C≡CCO_2Et)($Et_2PCH_2CH_2PEt_2$)$_2$][BPh_4]. J. Chem. Soc., Dalton Trans 1993, 391, 1841–1847.
28. Lenges CP; Brookhart M; Grant BE H/D exchange reactions between C_6D_6 and $C_5Me_5Co(CH_2{=}CHR)_2$ (R = H, $SiMe_3$): Evidence for oxidative addition of C(sp^2)-H bonds to the [C_5Me_5(L)Co] moiety. J. Organomet. Chem 1997, 528, 199–203.
29. Lenges CP; Brookhart M Co(I)-Catalyzed Inter- and Intramolecular Hydroacylation of Olefins with Aromatic Aldehydes. J. Am. Chem. Soc 1997, 119, 3165–3166.
30. Bolig AD; Brookhart M Activation of sp3 C—H Bonds with Cobalt(I): Catalytic Synthesis of Enamines. J. Am. Chem. Soc 2007, 129, 14544–14545. [PubMed: 17985901]
31. Sanjosé-Orduna J; Gallego D; Garcia-Roca A; Martin E; Benet-Buchholz J; Pérez-Temprano MH Capturing Elusive Cobaltacycle Intermediates: A Real-Time Snapshot of the Cp*CoIII-Catalyzed Oxidative Alkyne Annulation. Angew. Chem. Int. Ed 2017, 56, 12137–12141.
32. Lau W; Huffman JC; Kochi JK Electrochemical oxidation-reduction of organometallic complexes. Effect of the oxidation state on the pathways for reductive elimination of dialkyliron complexes. Organometallics 1982, 1, 155–169.
33. Joannou MV; Jonathan MDarmon JM; Bezdek MJ; Chirik PJ Exploring C(sp^3)-C(sp^3) reductive elimination from an isolable iron metallacycle. Polyhedron 2019, 159, 308–317.
34. Xu H; Bernskoetter WH Mechanistic considerations for C-C bond reductive coupling at a cobalt(III) center. J. Am. Chem. Soc 2011, 133, 14956–14959. [PubMed: 21895015]
35 (a). Bart SC; Lobkovsky E; Chirik PJ Preparation and molecular and electronic structures of iron(0) dinitrogen and silane complexs and their application to catalytic hydrogenation and hydrosilation. J. Am. Chem. Soc 2004, 126, 13794–13807. [PubMed: 15493939] (b)Archer AA; Bouwkamp MW; Cortez M-P; Lobkovsky E; Chirik PJ Arene coordination in bis(imino)pyridine iron complexes: Identification of catalyst deactivation pathways in iron-catalyzed hydrogenation and hydrosilation. Organometallics 2006, 25, 4269–4278.(c)Chirik PJ Iron- and cobalt-catalyzed alkene hydrogenation: Catalysis with both redox-active and strong field ligand. Acc. Chem. Res 2015, 48, 1687–1695. [PubMed: 26042837] (d)Zhang Z; Butt NA; Zhou M; Liu D; Zhang W Asymmetric transfer and pressure hydrogenation with earth-abundant transition metal catalysts. Chin. J. Chem 2018, 36, 443–454.
36 (a). Tondreau AM; Atienza CCH; Weller KJ; Nye SA; Lewis KM; Delis JGP; Chirik PJ Iron catalysts for selective anti-Markovnikov alkene hydrosilylation using tertiary silanes. Science 2012, 335, 567–570. [PubMed: 22301315] (b)Atienza CCH; Tondreau AM; Weller KJ; Lewis KM; Cruse RW; Nye SA; Boyer JL; Delis JGP; Chirik PJ High-selectivity bis(imino)pyridine iron catalysts for the hydrosilylation of 1,2,4-trivinylcyclohexane. ACS Catal. 2012, 10, 2169–2172.
37. Obligacion JV; Chirik PJ Highly selective bis(imino)pyridine iron-catalyzed alkene hydroboration. Org. Lett 2013, 15, 2680–2683. [PubMed: 23688021]
38. Bouwkamp MW; Bowman AC; Lobkovsky E; Chirik PJ Iron-catalyzed [2π+2π] cycloaddition of α,ω-dienes: The importance of redox-active supporting ligands. J. Am. Chem. Soc 2006, 128, 13340–13341. [PubMed: 17031930]
39. Russell SK; Lobkovsky E; Chirik PJ Iron-catalyzed intermolecular [2π+2π] cycloaddition J. Am. Chem. Soc 2011, 133, 8858–8861. [PubMed: 21598972]
40. Hoyt JM; Schmidt VA; Tondreau AM; Chirik PJ The iron-catalyzed intermolecular [2+2] cycloadditions of unactivated alkenes. Science 2015, 349, 960–963. [PubMed: 26315433]
41. Rummelt SM; Zhong H; Korobkov I; Chirik PJ Iron-mediated coupling of carbon dioxide and ethylene: Macrocyclic metallolactones enable access to various carboxylates. J. Am. Chem. Soc 2018, 140, 11589–11593. [PubMed: 30173506]
42. Darmon JM; Turner ZR; Lobkovsky E; Chirik PJ Electronic effects in 4-substituted bis(imino)pyridines and the corresponding reduced iron compounds. Organometallics 2012, 31, 2275–2285. [PubMed: 22675236]

Author Manuscript Author Manuscript Author Manuscript Author Manuscript

43 (a). Kubas GJ Metal Dihydrogen and σ-Bond Complexes: Structure, Theory and Reactivity. Springer, New York, 2001.(b)Crabtree RH Dihydrogen complexes & related sigma complexes. Encyclopedia of Inorganic and Bioinorganic Chemistry 2011, 1–6.

44. Trovitch RJ; Lobkovsky E; Bill E; Chirik PJ Functional group tolerance and substrate scope in bis(imino)pyridine iron catalyzed alkene hydrogenation. Organometallics 2008, 27, 1470–1478.

45. Trovitch RJ; Lobkovsky E; Bouwkamp MW; Chirik PJ Carbon-oxygen cleavage by bis(imino)pyridine iron compounds: Catalyst deactivation pathways and observation of acyl C-O bond cleavage in esters. Organometallics 2008, 27, 6264–6278.

46. Bowman AC; Milsmann C; Atienza CCH; Lobkovsky E; Wieghardt K; Chirik PJ Synthesis and molecular and electronic structures of reduced bis(imino)pyridine cobalt dinitrogen complexes: Ligand versus metal reduction. J. Am. Chem. Soc 2010, 132, 1676–1684. [PubMed: 20085321]

47. Schmidt VA; Hoyt JM; Margulieux GW; Chirik PJ Cobalt-catalyzed [2π+2π] cycloaddition of alkenes: Scope, mechanism, and elucidation of electronic structure of catalytic intermediates. J. Am. Chem. Soc 2015, 137, 7903–7914. [PubMed: 26030841]

48. Fernández I; Trovitch RJ; Lobkovsky E; Chirik PJ Synthesis of bis(imino)pyridine di- and monoalkyl complexes: Stability differences between $FeCH_2SiMe_3$ and $FeCH_2CMe_3$ derivatives. Organometallics 2008, 27, 109–118.

49. Zhu D; Korobkov I; Budzelaar PHM Radical mechanisms in the reaction of organic halides with diiminepyridine cobalt complexes. Organometallics 2012, 31, 3958–3971.

50. Alawisi H; Al-Afyouni KF; Arman HD; Tonzetich ZJ Aldehyde decarbonylation by a cobalt(I) pincer complex. Organometallics 2018, 37, 4128–4135.

51. Trovitch RJ; Lobkovsky E; Chirik PJ Bis(imino)pyridine iron alkyls containing β-hydrogens: Synthesis, evaluation of kinetic stability, and decomposition pathways involving chelate participation. J. Am. Chem. Soc 2008, 130, 11631–11640. [PubMed: 18686955]

52. Trovitch RJ; Lobkovsky E; Chirik PJ Bis(diisopropylphosphino)pyridine iron dicarbonyl, dihydride and silyl hydride complexes. Inorg. Chem 2006, 45, 7252–7260. [PubMed: 16933926]

53 (a). Maseras F; Duran M; Lledos A; Bertrán J Molecular hydrogen complexes with a hydride ligand. An ab initio study on the iron hydride, $[Fe(PR_3)_4H(H_2)]^+$, system. J. Am. Chem. Soc 1991, 113, 2879–2884.(b)Van Der Sluys LS; Eckert J; Eisenstein O; Hall JH; Huffman JC; Jackson SA; Koetzle TF; Kubas GJ; Vergamini PJ; Caulton KG An attractive cis-effect of hydride on neighbor ligands: experimental and theoretical studies on the structure and intramolecular rearrangements of $Fe(H)_2(\eta^2\text{-}H_2)(PEtPh_2)3$. J. Am. Chem. Soc 1990, 112, 4831–4841.(c)Bianchini C; Masi D; Peruzzini M; Casarin M; Maccato C; Rizzi GA *Ab Initio* and Experimental Studies on the Structure and Relative Stability of the *cis*-Hydride-η^2-Dihydrogen Complexes $[\{P(CH_2CH_2PPh_2)3\}M(H)(\eta^2\text{-}H_2)]^+$ (M = Fe, Ru). Inorg. Chem 1997, 36, 1061–1069. [PubMed: 11669669] (d)Jackson SA; Eisenstein O Conformation of hydrogen molecule on dinuclear complexes: attractive effect of a *cis* hydride. Inorg. Chem 1990, 29, 3910–3914.

54 (a). Gorgas N; Alves LG; Stöger B; Martins AM; Veiros LF; Kirchner K Stable, Yet Highly Reactive Non-classical Polyhydride Iron Pincer Complexes - Z-Selective Dimerization and Hydroboration of Terminal Alkynes J. Am. Chem. Soc 2017, 139, 8130–8133. [PubMed: 28586219] (b)Gorgas N; Stoger B; Veiros LF; Kirchner K Iron(II) (Bis)Acetylide Complexes as Key Intermediates in the Catalytic Hydrofunctionalization of Terminal Alkynes ACS Catal. 2018, 8, 7973–7983.

55. Danopoulos AA; Wright JA; Motherwell WB Molecular N_2 complexes of iron stabilised by *N*-heterocyclic'pincer' dicarbene ligands. Chem. Commun 2005, 784–786.

56 (a). Danopoulos AA; Pugh D; Smith H; Sassmannshausen J Structural and reactivity studies of "pincer" pyridine dicarbene complexes of Fe^0: Experimental and computational comparison of the phosphine and NHC donors. Chem. Eur. J 2009, 15, 5491–5502. [PubMed: 19373799] (b)Zhang X Theoretical study on electronic structure of (CNC)Fe_$2N_2$ and Its N_2 elimination mechanism. Int. J. Quant. Chem 2010, 110, 1880–1889.

57. Darmon JM; Yu RP; Semproni SP; Turner ZR; Stieber SCE; DeBeer S; Chirik PJ Electronic structure determination of pyridine N-heterocyclic carbene iron dinitrogen complexes and neutral ligand derivatives. Organometallics 2014, 33, 5423–5433. [PubMed: 25328270]

58. Stieber SCE; Milsmann C; Hoyt JM; Turner ZR; Finkelstein KD; Wieghardt K; DeBeer S; Chirik PJ Bis(imino)pyridine iron dinitrogen compounds revisited: Differences in electronic structure

Author Manuscript Author Manuscript Author Manuscript Author Manuscript

between four- and five-coordinate derivatives. Inorg. Chem 2012, 51, 3770–3785. [PubMed: 22394054]

59. Pugh D; Wells NJ; Evans DJ; Danopoulos AA Reactions of ‘pincer’ pyridine dicarbene complexes of Fe(0) with silanes. Dalton Trans. 2009, 7189–7195. [PubMed: 20449162]
60. Yu RP; Darmon JM; Hoyt JM; Margulieux GM; Turner ZR; Chirik PJ High-activity iron catalysts for the hydrogenation of hindered, unfunctionalized alkenes. ACS Catal. 2012, 2, 1760–1764. [PubMed: 26229734]
61. Yu RP; Hesk D; Rivera N; Pelczer I; Chirik PJ iron-catalyzed tritiation of pharmaceuticals. Nature 2016, 529, 195–199. [PubMed: 26762456]

62 (a). Nilsson GN; Kerr WJ The Development and Use of Novel Iridium Complexes as Catalysts for Ortho-Directed Hydrogen Isotope Exchange Reactions. J. Label Compd. Radiopharm 2010, 53, 662–667.(b)Brown JA; Cochrane AR; Irvine S; Kerr WJ; Mondal B; Parkinson JA; Paterson LC; Reid M; Tuttle T; Andersson S; Nilsson GN The Synthesis of Highly Active Iridium(I) Complexes and Their Application in Catalytic Hydrogen Isotope Exchange. Adv. Synth. Catal 2014, 356, 3551–3562.(c)Atzrodt J; Derdau V; Kerr WJ; Reid M C—H Functionalisation for Hydrogen Isotope Exchange. Angew. Chem. Int. Ed 2018, 57, 2–28.

63 (a). Isin EM; Elmore CS; Nilsson GN; Thompson RA; Weidolf L Use of Radiolabeled Compounds in Drug Metabolism and Pharmacokinetic Studies. Chemical Research in Toxicology 2012, 25, 532–542. [PubMed: 22372867] (b)Lockley WJS; McEwen A; Cooke R Tritium: a Coming of Age for Drug Discovery and Development ADME Studies. J. Labelled Compd. Radiopharm 2012, 55, 235–257.(c)Elmore CS; Bragg RA Isotope Chemistry; A Useful Tool in the Drug Discovery Arsenal. Bioorg. Med. Chem. Lett 2015, 25, 167–171. [PubMed: 25499878]

64 (a). Allen PH; Hickey MJ; Kingston LP; Wilkinson DJ Metal-Catalysed Isotopic Exchange Labelling: 30 Years of Experience in Pharmaceutical R&D. J. Labelled Compd. Radiopharm 2010, 53, 731–738.(b)Voges R; Heys JR; Moenius T Preparation of compounds labeled with tritium and carbon-14; Wiley: Chichester, UK, 2009.

65 (a). Atzrodt J; Derdau V; Kerr WJ; Reid M C—H Functionalisation for hydrogen Isotope Exchange. Angew. Chem., Int. Ed 2018, 57, 2–28.(b)Alero M; Burhop A; Jess K; Weck R; Tamm M; Atzrodt J; Derdau V Evaluation of a P,N- Ligated Iridium(I) Catalyst in Hydrogen Isotope Exchange Reactions of Aryl and Heteroaryl Compounds. J. Labelled Compd. Radiopharm 2018, 61, 380–385.(c)Kerr WJ; Lindsay DM; Owens PK; Reid M; Tuttle T; Campos S Site-Selective Deuteration of N- Heterocycles via Iridium-Catalyzed Hydrogen Isotope Exchange. ACS Catal. 2017, 7, 7182–7186.

66. Yu RP; Darmon JM; Semproni SP; Turner ZR; Chirik PJ Synthesis of Iron Hydride Complexes Relevant to Hydrogen Isotope Exchange in Pharmaceuticals. Organometallics 2017, 36, 4341–4343.

67 (a). Bedford RB, Brenner PB The development of iron catalysts for cross-coupling reactions. Top. Organomet. Chem 2015, 50, 19–46.(b)Bedford RB How low does iron go? Chasing the active species in Fe-catalyzed cross-coupling reactions. Acc. Chem. Res 2015, 48, 1485–1493. [PubMed: 25916260] (c)Daifuku SL; Kneebone JL; Snyder BER; Neidig ML Iron(II) active species in iron-bisphosphine catalyzed Kumada and Suzuki– Miyaura cross-couplings of phenyl nucleophiles and secondary alkyl halides. J. Am. Chem. Soc 2015, 137, 11432–11444. [PubMed: 26266698] (d)Crockett MP; Tyrol CC; Wong AS; Byers JA Iron-catalyzed Suzuki- Miyaura cross-coupling reactions between alkyl halides and unactivated arylboronic acids. Org. Lett 2018, 20, 5233–5237. [PubMed: 30132330] (e)O’Brien HM; Manzotti M; Abrams RD; Elorriaga D; Sparkes HA; Davis SA; Bedford RB Iron-catalysed substrate-directed Suzuki biaryl cross coupling. Nat. Catal 2018, 1, 429–437.(f)Wu GJ; Jacobi Von Wengelin A Iron-catalysed Suzuki biaryl couplings. Nat. Catal 2018, 1, 377–378.(g)Neidig ML; Carpenter SH; Curran DJ; DeMuth JC; Fleischauer VE; Ianuzzi TE; Neate PGN; Sears JD; Wolford NJ Development and evolution of mechanistic understanding in iron-catalyzed cross-coupling. Acc. Chem. Res 2019, 52, 140–150. [PubMed: 30592421] (h)Nakamura E; Hatakeyama T; Ito S; Ishizuka K; Ilies L; Nakamura M Iron-catalyzed Cross-coupling Reactions. Org. React 2014, 83, 1–209.(i)Sherry BD; Fürstner A The Promise and Challenge of Iron-Catalyzed Cross Coupling. Acc. Chem. Res 2008, 41, 1500–1511. [PubMed: 18588321] (j)Piontek A; Bisz E; Szostak M Iron-Catalyzed Cross-Couplings in the Synthesis of Pharmaceuticals: In Pursuit of Sustainability. Angew. Chem. Int. Ed 2018, 57, 11116–11128.(k)Clemancey M; Cantat T; Blondin G; Latour J-M; Dorlet P;

Author Manuscript Author Manuscript Author Manuscript Author Manuscript

Lefevre G Structural Insights into the Nature of Fe0 and FeI Low-Valent Species Obtained upon the Reduction of Iron Salts by Aryl Grignard Reagents. Inorg. Chem 2017, 56, 3834–3848. [PubMed: 28294603]

68. Blom B; Tan G; Enthaler S; Inoue S; Epping JD; Driess M Bis-N-Heterocyclic Carbene (NHC) Stabilized η^6-Arene Iron(0) Complexes: Synthesis, Structure, Reactivity, and Catalytic Activity. J. Am. Chem. Soc 2013, 135, 18108–1812. [PubMed: 24195449]

69 (a). Monfette S; Turner ZR; Semproni SP; Chirik PJ Enantiopure C1 symmetric bis(imino)pyridine cobalt complexes for asymmetric alkene hydrogenation. J. Am. Chem. Soc 2012, 134, 4561–4564. [PubMed: 22390262] (b)Friedfeld MR; Shevlin M; Margulieux GW; Campeau LC; Chirik PJ Cobalt-catalyzed enantioselective hydrogenation of minimally functionalized alkenes: Isotopic labeling provides insight into the origin of stereoselectivity and alkene insertion preferences. J. Am. Chem. Soc 2016, 138, 3314–3324. [PubMed: 26854359]

70 (a). Friedfeld MR; Margulieux GW; Schaefer BA; Chirik PJ Bis(phosphine)cobalt dialkyl complexes for directed catalytic alkene hydrogenation. J. Am. Chem. Soc 2014, 136, 13178–13181. [PubMed: 25166760] (b)Friedfeld MR; Shevlin M; Hoyt JM; Krska SW; Tudge MT Cobalt precursors for high-throughput discovery of base metal asymmetric alkene hydrogenation. Science 2013, 342, 1076–1080. [PubMed: 24288328] (c)Friedfeld MR; Zhong HY; Ruck RT; Shevlin M; Chirik PJ Cobalt-catalyzed asymmetric hydrogenation of enamides enabled by single electron reduction. Science 2018, 360, 888–892. [PubMed: 29798879]

71. Ma X; Lei M Mechanistic insights into the directed hydrogenation of hydroxylated alkene catalyzed by bis(phosphine)cobalt dialkyl complexes. J. Org. Chem 2017, 82, 2703–2712. [PubMed: 28195727]

72. Hopmann KH Cobalt bis(imino)pyridine-catalyzed asymmetric hydrogenation: Electronic structure, mechanism and stereoselectivity. Organometallics 2013, 32, 6388–6399.

73. Morello GR; Zhong HY; Chirik PJ; Hopmann KH Cobalt-catalysed alkene hydrogenation: A metallacycle can explain the hydroxyl activating effect and the diastereoselectivty. Chem. Sci 2018, 9, 4977–4982. [PubMed: 29938025]

74. Zhong H; Friedfeld MR; Camacho-Bunquin J; Sohn H; Yang C; Delfarro M; Chirik PJ Exploring the alcohol stability of bis(phosphine) cobalt dialkyl precatalysts in asymmetric alkene hydrogenation. Organometallics 2019, 38, 149–156.

75. Yang J; Seto YW; Yoshikai N Cobalt-Catalyzed Intermolecular Hydroacylation of Olefins Through Chelation-Assisted Imidoyl C—H Activation. ACS Catalysis 2015, 5, 3054–3057.

76. Kim DK; Riedel J; Kim RS; Dong VM Cobalt Catalysis for Enantioselective Cyclobutanone Construction. J. Am Chem. Soc 2017, 139, 10208–10211. [PubMed: 28704053]

77. Gandeepan P; Muller TZ; Zell D; Cera G; Warratz S; Ackermann L 3d transition metals for C—H activation. Chem. Rev 2019, 119, 2192–2452. [PubMed: 30480438]

78. Bowman AC; Milsmann C; Bill E; Lobkovsky E; Weyhermüller T; Wieghardt K; Chirik PJ Reduced N-Alkyl Substituted Bis(Imino)Pyridine Cobalt Complexes: Molecular and Electronic Structures for Compounds Varying by Three Oxidation States. Inorg. Chem 2010, 49, 6110–6123. [PubMed: 20540554]

79. Knijnenburg Q; Horton AD; van der Heijden H; Kooistra TM; Hetterscheid DGH; Smits JMM; de Bruin B; Budzelaar PHM; Gal AW Olefin hydrogenation using diimine pyridine complexes of Co and Rh. J. Mol. Cat. A: Chem 2005, 232, 151–159.

80. Obligacion JV; Chirik PJ Bis(imino)pyridine cobalt-catalyzed alkene isomerization-hydroboration: A strategy for remote hydrofunctionalization with terminal selectivity. J. Am. Chem. Soc 2013, 135, 19107–19110. [PubMed: 24328236]

81. Schuster CH; Diao T; Pappas I; Chirik PJ Bench-stable, substrate activated cobalt carboxylate pre-catalysts for alkene hydrosilylation with tertiary silanes. ACS *Catal.* 2016, 6, 2632–2636.

82. Atienza CCH; Diao TN; Weller KJ; Nye SA; Lewis KM; Delis JGP; Boyer JL; Roy AK; Chirik PJ Bis(imino)pyridine cobalt-catalyzed dehydrogenative silylation of alkenes: Scope, mechanism and origins of selective allylsilane formation. J. Am. Chem. Soc 2014, 136, 12108–12118. [PubMed: 25068530]

83 (a). Sun J; Deng L Cobalt complex-catalyzed hydrosilylation of alkenes and alkynes. ACS Catal. 2016, 6, 290–300.(b)Ai W; Zhong R; Liu X; Liu Q Hydride Transfer Reactions Catalyzed by

Author Manuscript Author Manuscript Author Manuscript Author Manuscript

Cobalt Complexes. Chem. Rev 2019, 119, 2876–2953. [PubMed: 30565455] (c)Mukherjee A; Milstein D Homogeneous catalysis by cobalt and manganese pincer complexes. ACS Catal, 2018, 8, 11435–11469.(d)Chen J; Lu Z Asymmetric Hydrofunctionalization of Minimally Functionalized Alkenes via Earth Abundant Transition Metal Catalysis. Org. Chem. Front 2018, 5, 260–272.(e)Du X; Huang Z Advances in Base-Metal-Catalyzed Alkene Hydrosilylation. ACS Catal. 2017, 7, 1227–1243.

84. Yu RP; Darmon JM; Milsmann C; Margulieux GW; Stieber SCE; DeBeer S; Chirik PJ Catalytic Hydrogenation Activity and Electronic Structure Determination of Bis(Arylimidazol-2-Ylidene)Pyridine Cobalt Alkyl and Hydride Complexes. J. Am. Chem. Soc 2013, 135, 13168–13184. [PubMed: 23968297]

85. Khaskin E; Diskin-Posner Y; Weiner L; Leitus G; Milstein D Formal loss of an H radical by a cobalt complex via metal-ligand cooperation. Chem. Commun 2013, 49, 2771–2773.

86. Obligacion JV; Semproni SP; Chirik PJ Cobalt-Catalyzed C—H Borylation. J. Am. Chem. Soc 2014, 136, 4133–4136. [PubMed: 24588541]

87. Semproni SP; Hojilla Atienza CC; Chirik PJ Oxidative Addition and C—H Activation Chemistry with a PNP Pincer-Ligated Cobalt Complex. Chem. Sci 2014, 5, 1956–1960.

88. Semproni SP; Milsmann C; Chirik PJ Four-Coordinate Cobalt Pincer Complexes: Electronic Structure Studies and Ligand Modification by Homolytic and Heterolytic Pathways. J. Am. Chem. Soc 2014, 136, 9211–9224. [PubMed: 24897302]

89. Bezdek M, Guo S; Chirik PJ Coordination induced bond weakening of ammonia, water, and hydrazine with a molybdenum complex. Science 2016, 354, 730–733. [PubMed: 27846601]

90 (a). C—H bond activation by rhodium(I) hydroxide and phenoxide complexes. Kloek SM; Heinekey DM; Goldberg KI Angew. Chem. Int. Ed 2007, 46, 4736–4738.(b)C—H Bond Activation by Rhodium(I) Phenoxide and Acetate Complexes: Mechanism of H—D Exchange between Arenes and Water. Kloek SM; Heinekey DM; Goldberg KI Organometallics 2008, 27, 1454–1463.

91 (a). Schwartsburd L; Iron MA; Konstantinovski L; Ben-Ari E; Milstein D A dearomatized anionic PNP pincer rhodium complex: C-H and H—H bond activation by metal-ligand cooperation and inhibition by dinitrogen. Organometallics 2011, 30, 2721–2729.(b)Anaby A; Feller M; Ben-David Y; Leitus G; Diskin-Posner Y; Shimon LJW; Milstein D Bottom-Up Construction of a CO2-Based Cycle for the Photo-carbonylation of Benzene, Promoted by a Rhodium(I) Pincer Complex. J. Am. Chem. Soc 2016, 138, 9941–9950. [PubMed: 27400288]

92. Scheuermann ML; Semproni SP; Pappas I; Chirik PJ Carbon Dioxide Hydrosilylation Promoted by Cobalt Pincer Complexes. Inorg. Chem 2014, 53, 9463–9465. [PubMed: 25171221]

93. Neely JM, Bezdek MJ; Chirik PJ Insight into Transmetalation Enables Cobalt-Catalyzed Suzuki-Miyaura Cross Coupling. ACS Cent. Sci 2016, 2, 935–942. [PubMed: 28058283]

94. Rummelt SM; Zhong H; Leonard NG; Semproni SP; Chirik PJ Oxidative Addition of Dihydrogen, Boron Compounds, and Aryl Halides to a Cobalt(I) Cation Supported by a Strong-Field Pincer Ligand. Organometallics, 2019, 38, 1081–1090. [PubMed: 30962670]

95. Tokmic K; Markus CR; Zhu L; Fout AR Well-Defined Cobalt(I) Dihydrogen Catalyst: Experimental Evidence for a Co(I)/Co(III) Redox Process in Olefin Hydrogenation. J. Am. Chem. Soc 2016, 138, 11907–11913. [PubMed: 27569420]

96 (a). Ibrahim AD; Entsminger SW; Fout AR Insights into a Chemoselective Cobalt Catalyst for the Hydroboration of Alkenes and Nitriles. ACS Catal. 2017, 7, 3730–3734.(b)Ibrahim AD; Entsminger SW; Zhu L; Fout AR A Highly Chemoselective Cobalt Catalyst for the Hydrosilylation of Alkenes using Tertiary Silanes and Hydrosiloxanes. ACS Catal. 2016, 6, 3589–3593.

97. Hall DG; Boronic acids; Wiley-VCH: Weinheim, Germany, 2005.

98. Mkhalid IAI; Barnard JH; Marder TB; Murphy JM; Hartwig JF C—H Activation for the Construction of C—B Bonds. Chem. Rev 2010, 110, 890–931. [PubMed: 20028025]

99. Hartwig JF Borylation and Silylation of C—H Bonds: a Platform for Diverse C—H Bond Functionalizations. Acc. Chem. Res 2012, 45, 864–873. [PubMed: 22075137]

100 (a). Cho J-Y; Tse MK; Holmes D; Maleczka RE; Smith MR Remarkably Selective Iridium Catalysts for the Elaboration of Aromatic C-H Bonds. Science 2002, 295, 305–308. [PubMed:

Author Manuscript Author Manuscript Author Manuscript Author Manuscript

11719693] (b)Ishiyama T; Takagi J; Ishida K; Miyaura N; Anastasi NR; Hartwig JF Mild Iridium-Catalyzed Borylation of Arenes. High Turnover Numbers, Room Temperature Reactions, and Isolation of a Potential Intermediate. J. Am. Chem. Soc 2002, 124, 390–391. [PubMed: 11792205] (c)Boller TM; Murphy JM; Hapke M; Ishiyama T; Miyaura N; Hartwig JF Mechanism of the Mild Functionalization of Arenes by Diboron Reagents Catalyzed by Iridium Complexes. Intermediacy and Chemistry of Bipyridine-Ligated Iridium Trisboryl Complexes. J. Am. Chem. Soc 2005, 127, 14263–14278. [PubMed: 16218621] (d)Tamura H; Yamazaki H; Sato H; Sakaki S Iridium-Catalyzed Borylation of Benzene with Diboron. Theoretical Elucidation of Catalytic Cycle Including Unusual Iridium(v) Intermediate. J. Am. Chem. Soc 2003, 125, 16114–16126. [PubMed: 14678004] (e)Green AG; Liu P; Merlic CA; Houk KN Distortion/Interaction Analysis Reveals the Origins of Selectivities in Iridium-Catalyzed C—H Borylation of Substituted Arenes and 5-Membered Heterocycles. J. Am. Chem. Soc 2014, 136, 4575–4583. [PubMed: 24580415]

101. Obligacion JV; Semproni SP; Pappas I; Chirik PJ Cobalt-Catalyzed C(sp^2)-H Borylation: Mechanistic Insights Inspire Catalyst Design. J. Am. Chem. Soc 2016, 138, 10645–10653. [PubMed: 27476954]
102. Obligacion JV; Chirik PJ Mechanistic Studies of Cobalt-Catalyzed C(sp^2)—H Borylation of Five-Membered Heteroarenes with Pinacolborane. ACS Catal. 2017, 7, 4366–4371. [PubMed: 29479489]
103. Li H; Obligacion JV; Chirik PJ; Hall MB Cobalt Pincer Complexes in Catalytic C—H Borylation: the Pincer Ligand Flips Rather Than Dearomatizes. ACS Catal. 2018, 8, 10606–10618. [PubMed: 30719402]
104. Obligacion JV; Bezdek MJ; Chirik PJ C(sp^2)—H Borylation of Fluorinated Arenes Using an Air-Stable Cobalt Precatalyst: Electronically Enhanced Site Selectivity Enables Synthetic Opportunities. J. Am. Chem. Soc 2017, 139, 2825–2832. [PubMed: 28139907]
105. Wang J; Sanchez-Rosello M; Acena JL; del Pozo C; Sorochinsky AE; Fustero S; Soloshonok VA; Liu H Fluorine in Pharmaceutical Industry: Fluorine-Containing Drugs Introduced to the Market in the Last Decade (2001–2011). Chem. Rev 2014, 114, 2432–2506. [PubMed: 24299176]
106. Fujiwara T; O'Hagan D Successful fluorine-containing herbicide agrochemicals. J. Fluorine Chem 2014, 167, 16–29.
107. Scheuermann ML; Johnson EJ; Chirik PJ Alkene isomerization-hydroboration promoted by phosphine-ligand cobalt catalysts. Org. Lett 2015, 17, 2716–2719. [PubMed: 26010715]
108. Noda D; Tahara A; Sunada Y; Nagashima H Non-precious metal catalytic systems involving iron and cobalt carboxylates and alkyl isocyanides for hydrosilylation of alkenes with hydrosiloxanes. J. Am. Chem. Soc 2016, 138, 2480–2483. [PubMed: 26760915]
109. Yang H; Zarate C; Palmer WN; Rivera N; Hesk D; Chirik PJ Site-Selective Nickel-Catalyzed Hydrogen Isotope Exchange in N-Heterocycles and Its Application to the Tritiation of Pharmaceuticals. ACS Catal. 2018, 8, 10210–10218.
110. Obligacion JV; Zhong H; Chirik PJ Insights Into Activation of Cobalt Pre-Catalysts for C(sp^2)—H Functionalization. Isr. J. Chem 2017, 57, 1032–1036. [PubMed: 29456261]
111. Léonard NG; Bezdek MJ; Chirik PJ Cobalt-Catalyzed C(sp^2)—H Borylation with an Air-Stable, Readily Prepared Terpyridine Cobalt(II) Bis(Acetate) Precatalyst. Organometallics 2017, 36, 142–150.
112. Schaefer BA; Margulieux GW; Small BL; Chirik PJ Evaluation of Cobalt Complexes Bearing Tridentate Pincer Ligands for Catalytic C—H Borylation. Organometallics 2015, 34, 1307–1320.
113. Zhang L; Zuo Z; Leng X; Huang Z A cobalt-catalyzed alkene hydroboration with pinacolborane. Angew. Chem. Int. Ed 2014, 53, 2696–2700.
114. Wang J; Hanan GS A Facile Route to Sterically Hindered and Non-Hindered 4′-Aryl-2,2′:6′,2″-Terpyridines. Synlett 2005, 8, 1251–1254.
115. Ren H; Zhou Y-P; Bai Y; Cui C; Driess M Cobalt-Catalyzed Regioselective Borylation of Arenes: N-Heterocyclic Silylene as an Electron Donor in the Metal-Mediated Activation of C—H Bonds. Chem. Eur. J 2017, 23, 5663–5667. [PubMed: 28229494]
116. Palmer WN; Chirik PJ Cobalt-Catalyzed Stereoretentive Hydrogen Isotope Exchange of C(sp^3)—H Bonds. ACS Catal. 2017, 7, 5674–5678. [PubMed: 29456876]

Author Manuscript Author Manuscript Author Manuscript Author Manuscript

117. Palmer WN; Obligacion JV; Pappas I; Chirik PJ Cobalt-Catalyzed Benzylic Borylation: Enabling Polyborylation and Functionalization of Remote, Unactivated C(sp^3)—H Bonds. J. Am. Chem. Soc 2016, 138, 766–769. [PubMed: 26714178]

118. Jayasundara CRK; Sabasovs D; Staples RJ; Oppenheimer J; Smith MR III, Maleczka RE Cobalt-catalyzed C-H borylation of alkyl arenes and heteroarenes including the first selective borylations of secondary benzylic C-H bonds. Organometallics 2018, 37, 1567–1574.

119 (a). Krska SW; DiRocco DA; Dreher SD; Shevlin M The evolution of chemical high-throughput experimentation to address challenging problems in pharmaceutical synthesis. Acc. Chem. Res 2017, 50, 2976–2985. [PubMed: 29172435] (b)Shevlin M Practical high-throughput experimentation for chemists. ACS Med. Chem. Lett 2017, 8, 601–607. [PubMed: 28626518]

120. Fürstner A; Martin R; Krause H; Seidel G; Goddard R; Lehmann CW Preparation, Structure, and Reactivity of Nonstabilized Organoiron Compounds. Implications for Iron-Catalyzed Cross Coupling Reactions. J. Am. Chem. Soc 2008, 130, 8773–8787. [PubMed: 18597432]

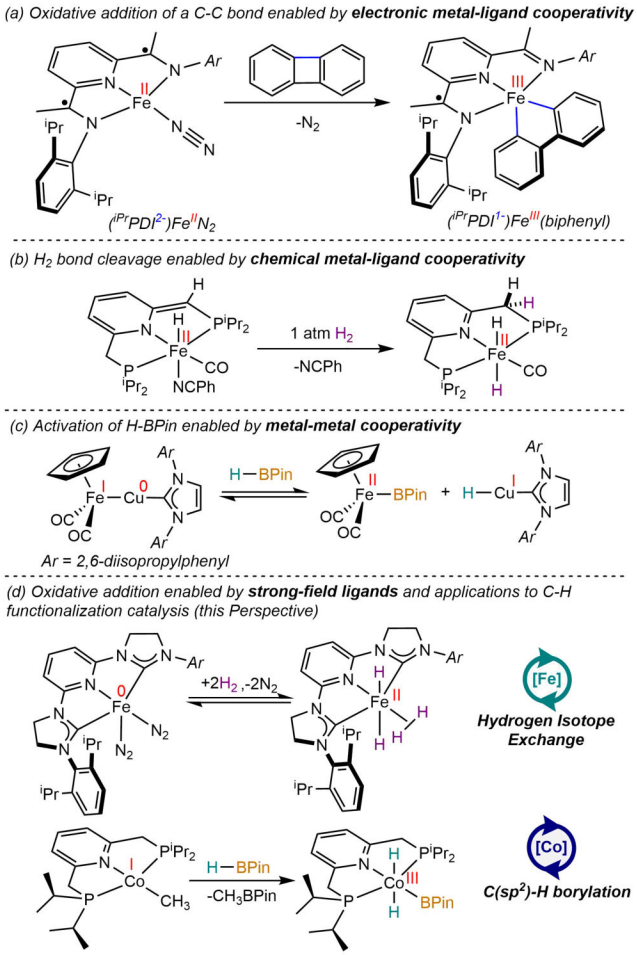

Scheme 1.

Strategies for enabling two-electron chemistry with first-row transition metals. (a) Reference 7, (b) reference 9d, (c) reference 10b, (d) references 61 and 81 for iron and cobalt, respectively.

Author Manuscript Author Manuscript Author Manuscript Author Manuscript

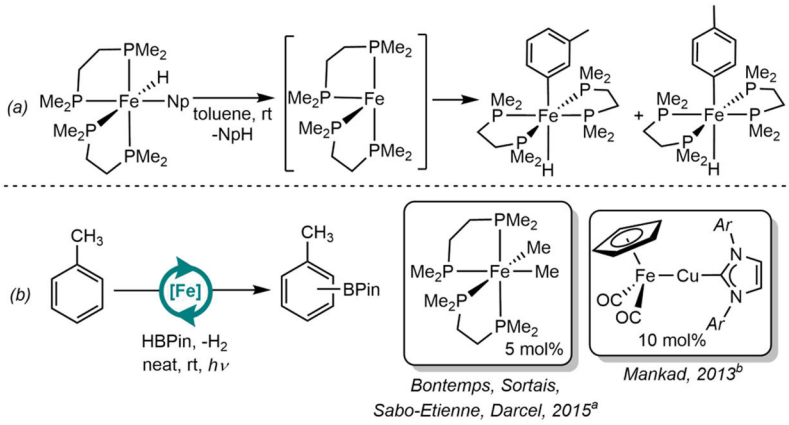

Scheme 2.

(a) A seminal example of C—H oxidative addition with reduced iron phosphine complex (Reference 18c), Np = 2-naphtyl. (b) First examples of catalytic C(sp^2)—H borylation of toluene by iron complexes: [a]Reference 20. Conditions: 72 h, UV (350 nm). 34% yield, 60:40 (*m:p*). [b]Reference 10a, Conditions: 24 h, 450-W Hg lamp. 83% yield, 62:38 (*m:p*).

Author Manuscript Author Manuscript Author Manuscript Author Manuscript

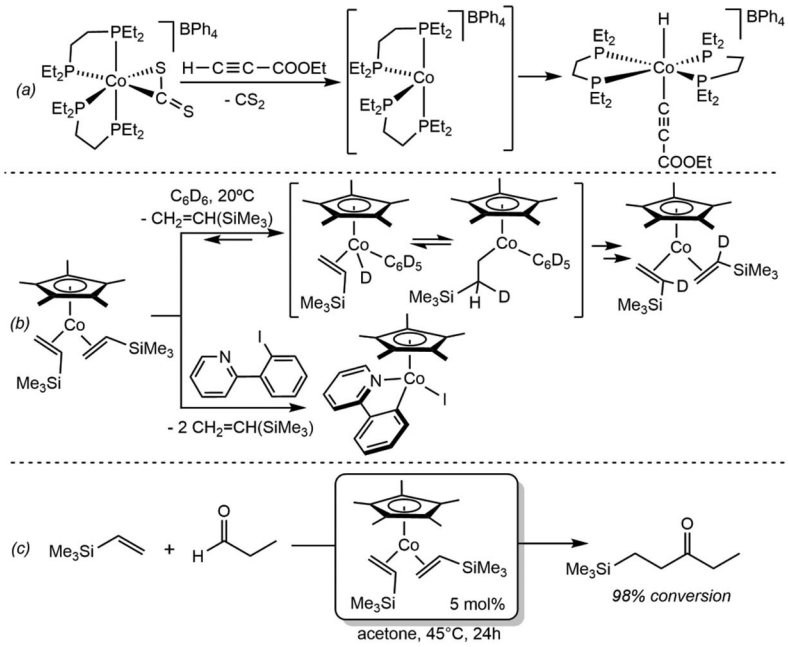

Scheme 3.

(a) An early example of alkyne C—H oxidative addition to Co(I) (reference 27), (b) (Top) C—D oxidative addition of benzene-d6 by (η^5-C_5Me_5)Co(CH_2=$CHSiMe_3$)$_2$ resulting on H/D exchange (reference 28), and (bottom) contemporary C—I oxidative addition to (η^5-C_5Me_5)Co(CH_2=$CHSiMe_3$)$_2$ and isolation of the resulting cyclopentadienyl cobalt (III) complex (reference 31). (c) Catalytic hydroacylation of vinyltrimethylsilane employing (η^5-C_5Me_5)Co(CH_2=$CHSiMe_3$)$_2$ as precatalyst (reference 29).

Author Manuscript Author Manuscript Author Manuscript Author Manuscript

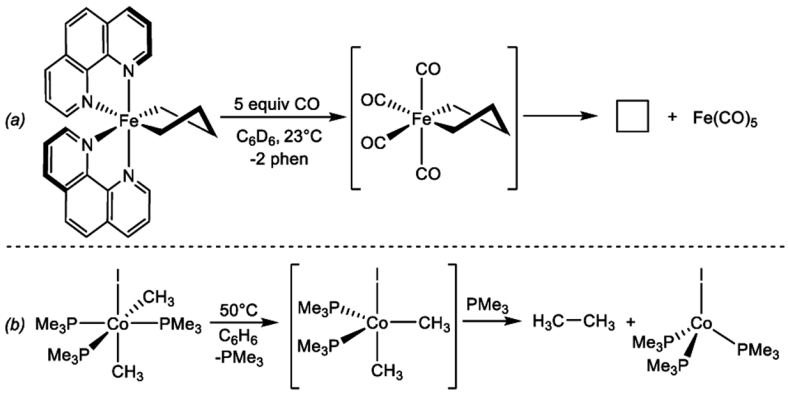

Scheme 4.

C—C reductive elimination from (a) an iron ferracyclopentane upon CO addition (reference 33) and (b) a cobalt (III) complex under thermal conditions (reference 34).

Author Manuscript Author Manuscript Author Manuscript Author Manuscript

Author Manuscript Author Manuscript Author Manuscript Author Manuscript

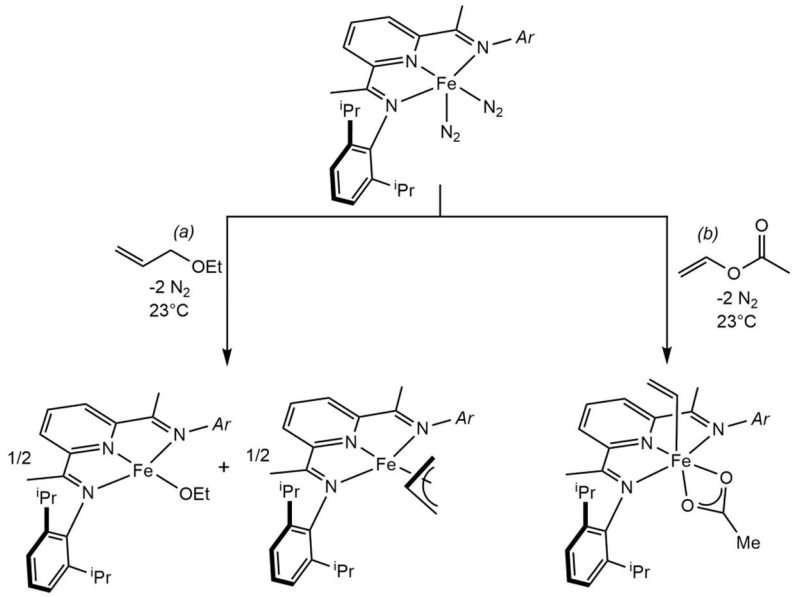

Scheme 5.

(a) Net 2-electron oxidative addition of an allyl ether over two iron centers to yield a mixture of an iron ethoxide and an iron allyl complex (reference 45). (b) C—O bond cleavage by oxidative addition of vinyl acetate on iron(0) (reference 45).

Author Manuscript Author Manuscript Author Manuscript Author Manuscript

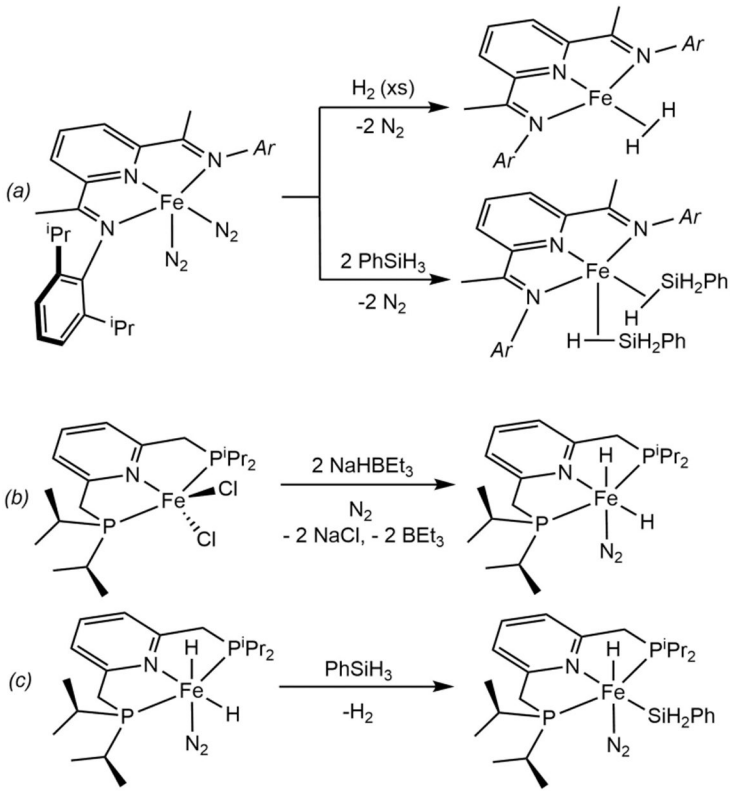

Scheme 6.

(a) Reaction of (^{iPr}PDI)Fe(N_2)$_2$ with H_2 (top) and $PhSiH_3$ (bottom) (reference 35a). (b) Synthesis of (^{iPr}PNP)FeH_2(N_2) (reference 52). (c) Oxidative addition of a Si-H bond of $PhSiH_3$ by (^{iPr}PNP)FeH_2(N_2) (reference 52).

Author Manuscript Author Manuscript Author Manuscript Author Manuscript

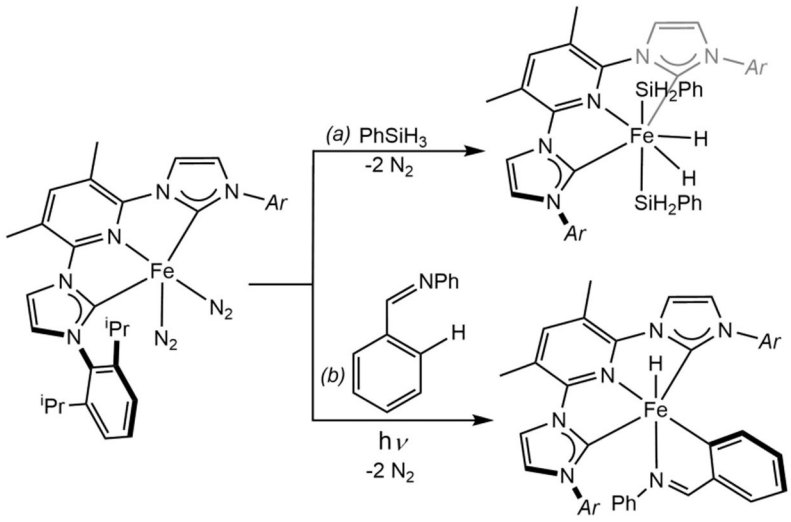

Scheme 7.

Oxidative addition promoted by (^{iPr}CNC)Fe(N_2)$_2$ of (a) the Si—H bond of SiH_3Ph (reference 59), and (b) the *ortho* C—H bond of benzaldehyde anilide upon UV irradiation (reference 59).

Author Manuscript Author Manuscript Author Manuscript Author Manuscript

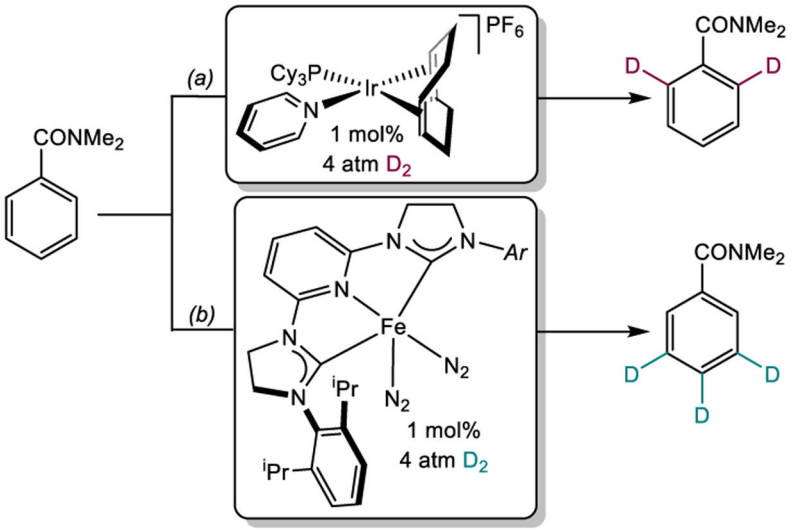

Scheme 8.

HIE with *N,N*-dimethylbenzamide catalyzed by (a) [Ir(COD)(pyridine)(PCy_3)]PF_6 (reference 61). Conditions: 23°C, CH_2Cl_2, 24 h. (b) (H_4-^{i}PrCNC)Fe(N_2)$_2$ (reference 61). Conditions: 45°C, THF, 24 h.

Author Manuscript Author Manuscript Author Manuscript Author Manuscript

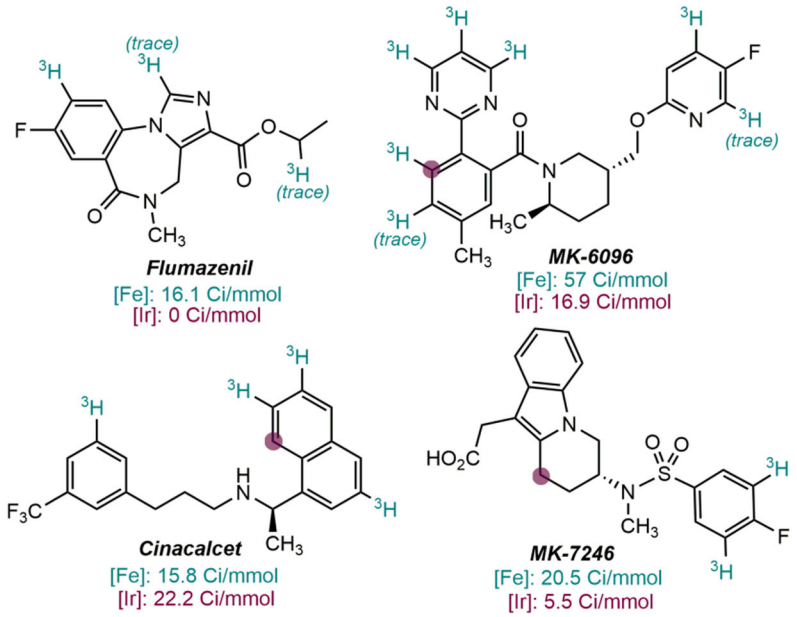

Scheme 9.

Drugs tritiated with (H_4-$^{i\text{Pr}}$CNC)Fe(N_2)$_2$ (reference 61). Positions labelled with [Ir(COD)(pyridine)(PCy_3)]PF_6 are highlighted with a purple dot. Specific activities are reported in green for Fe and red for Ir below each drug. Conditions for (H_4-$^{i\text{Pr}}$CNC)Fe(N_2)$_2$: 25 mol% catalyst loading, 7 μmol substrate, 1.2 Ci $^3H_2$ (0.15 atm), 0.2 ml NMP, 23 °C, 16 h. Conditions for [Ir(COD)(pyridine)(PCy_3)]PF_6: 25 mol% catalyst loading, 7 μmol substrate, 1.2 Ci $^3H_2$ (0.15 atm), 0.5 ml CH_2Cl_2, 23 °C, 16 h. The sodium salt conjugate base was used for the tritiation of MK-7246 owing to incompatibility of the carboxylic acid functionality with (H_4-$^{i\text{Pr}}$CNC)Fe(N_2)$_2$.

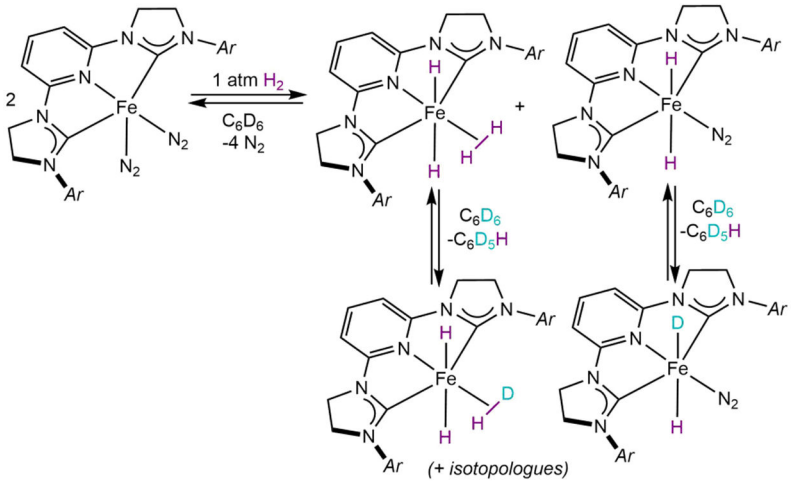

Scheme 10.

Reaction of $(H_4\text{-}^{i\text{Pr}}CNC)Fe(N_2)_2$ with H_2 and subsequent C—D activation of C_6D_6 (reference 66).

Author Manuscript Author Manuscript Author Manuscript Author Manuscript

Author Manuscript Author Manuscript Author Manuscript Author Manuscript

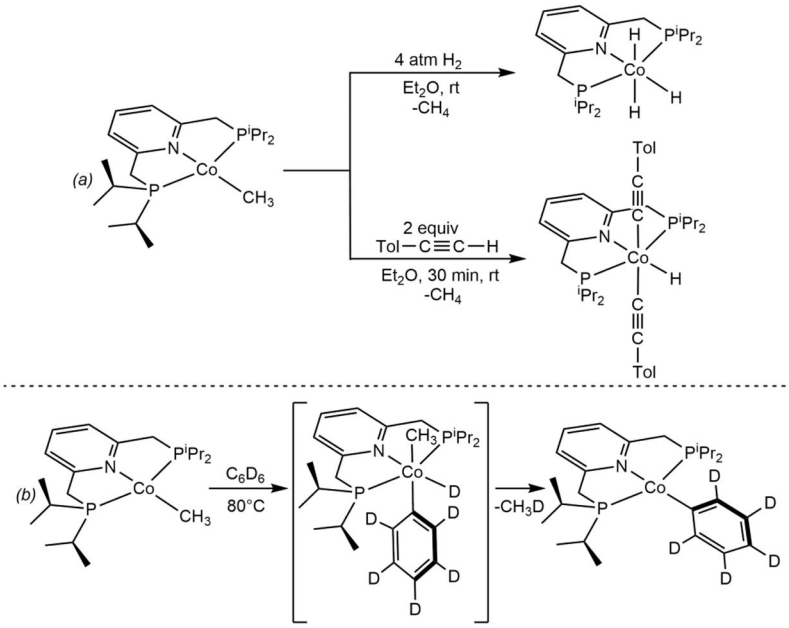

Scheme 11.

Oxidative addition of (a) H_2 and a C(sp)—H bond to (^{iPr}PNP)CoCH_3 to yield the corresponding cobalt(III) products (reference 87), and (b) the C(sp^2)—D bond of C_6D_6 affording a Co(I) phenyl complex (reference 87).

Author Manuscript Author Manuscript Author Manuscript Author Manuscript

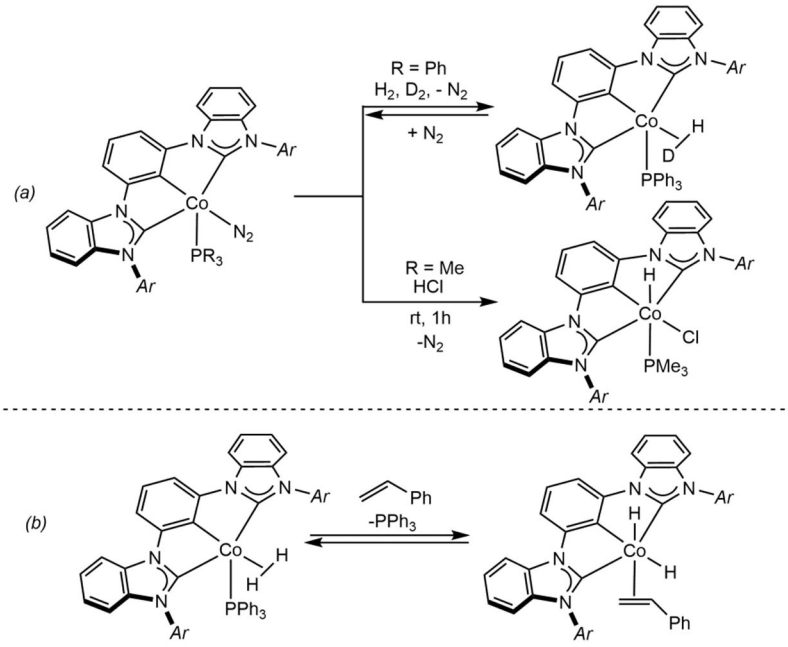

Scheme 12.

(a) H—D exchange between H_2 and D_2 enabled by (^{Mes}CCC)CoN_2(PPh_3) and HCl oxidative addition to ($^{Mes-}$ CCC)CoN_2(PMe_3) (reference 95), (b) oxidative addition of H_2 upon styrene coordination as a key step in olefin hydrogenation catalyzed by (^{Mes}CCC)CoN_2(PPh_3). *Ar* = 2,4,6-trimethylphenyl (reference 95).

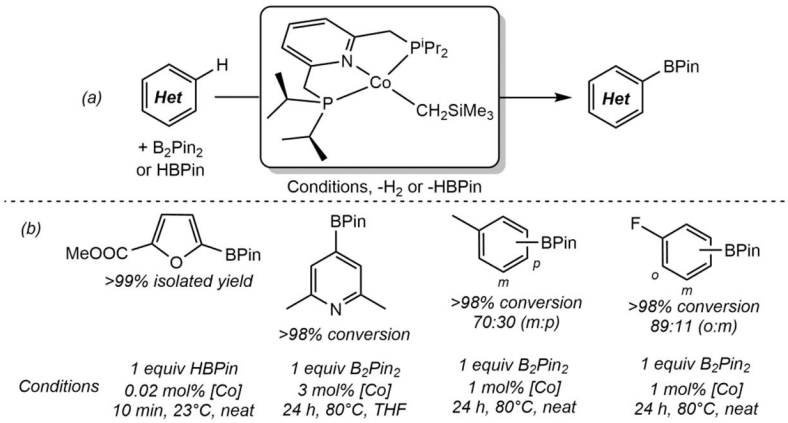

Scheme 13.

(a) Borylation of C(sp^2)—H bonds catalyzed by (^{iPr}PNP)CoCH_2SiMe_3 (reference 86), and (b) selected substrate scope (reference 86).

Author Manuscript Author Manuscript Author Manuscript Author Manuscript

Author Manuscript Author Manuscript Author Manuscript Author Manuscript

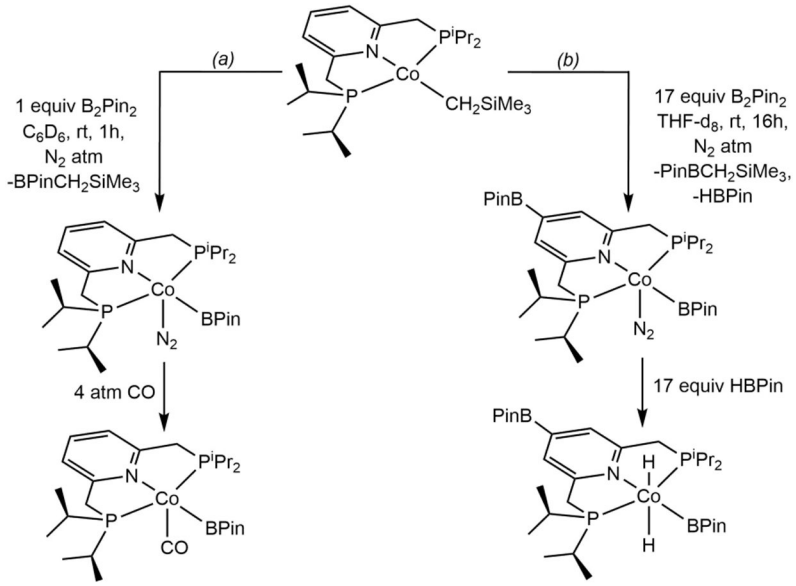

Scheme 14.

Reaction of (^{iPr}PNP)CoCH_2SiMe_3 with (a) the equimolar amount of B_2Pin_2 and subsequent addition of CO (reference 101) and (b) excess B_2Pin_2 and subsequent oxidative addition of HBPin (reference 101).

Author Manuscript Author Manuscript Author Manuscript Author Manuscript

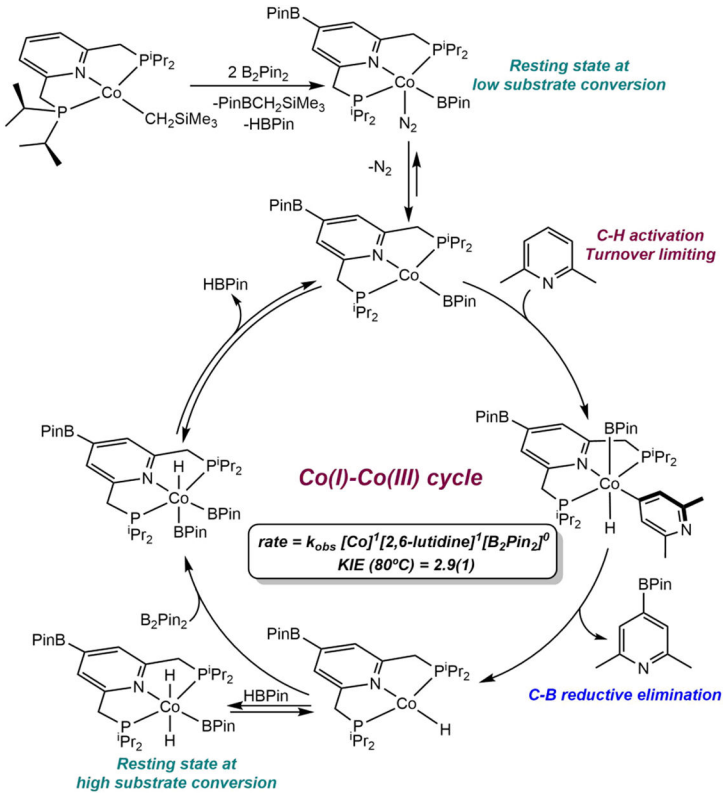

Scheme 15.

Mechanism of catalytic borylation of 2,6-lutidine with B_2Pin_2 catalyzed by (^{iPr}PNP)CoCH_2SiMe_3(reference 101).

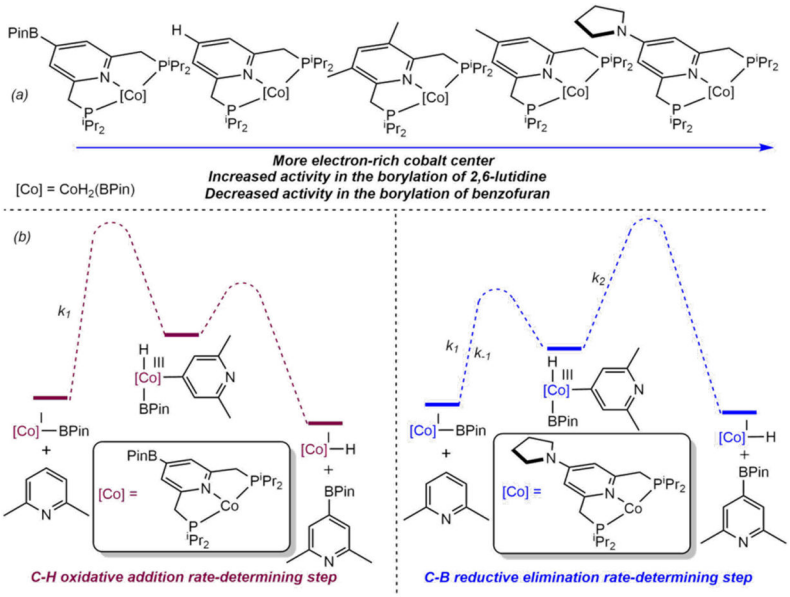

Scheme 16.

(a) Second-generation [(4-R-^{iPr}PNP)Co] borylation catalysts (reference 96), (b) Relevance of pincer electron-donating ability on the reaction coordinate (qualitative) of the 2,6-lutidine catalytic borylation (reference 101).

Author Manuscript Author Manuscript Author Manuscript Author Manuscript

Author Manuscript Author Manuscript Author Manuscript Author Manuscript

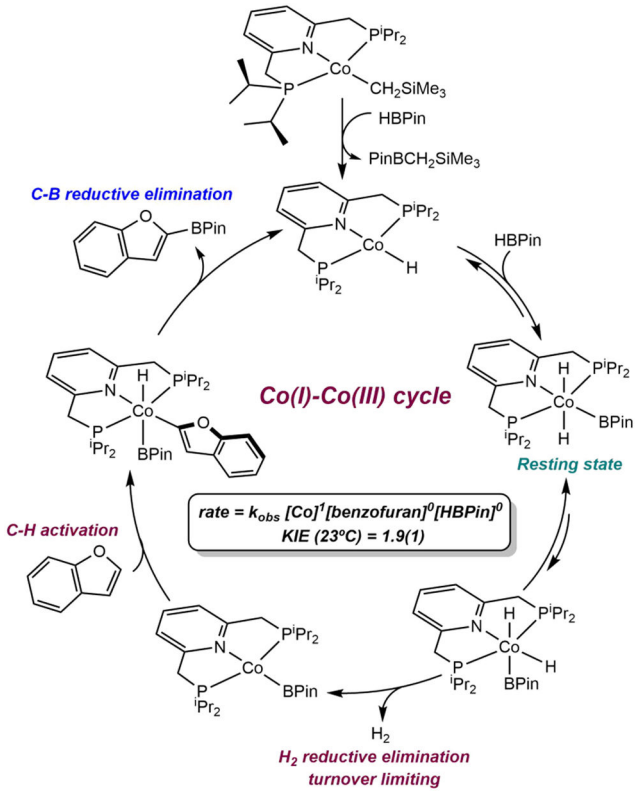

Scheme 17.

Mechanism of catalytic borylation of 2-methylfuran with HBPin employing (^{iPr}PNP)CoCH$_2$SiMe$_3$ as precatalyst (reference 102).

Author Manuscript Author Manuscript Author Manuscript Author Manuscript

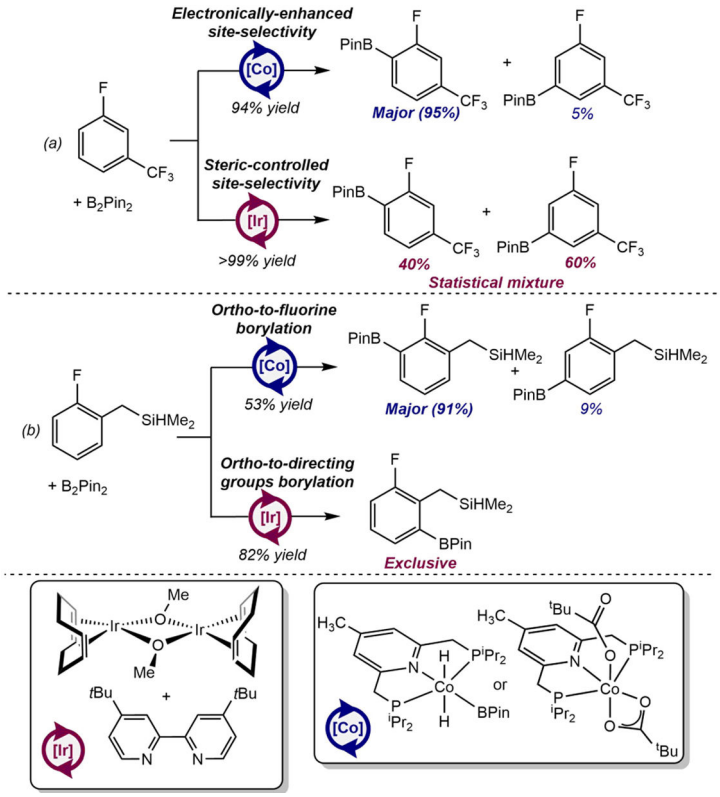

Scheme 18.

Highly selective *ortho*-to-fluorine borylation of (a) 3-fluorobenzotrifluoride and (b) 1-[(dimethylsilyl)methyl]-2-fluorobenzene catalyzed by (4-Me-^{iPr}PNP)CoH_2(BPin) or (4-Me-^{iPr}PNP)$Co(O_2CtBu)_2$ and comparison to the state-of-the-art iridium catalysis (reference 104). Conditions: (a) Cobalt: 5 mol% (4-Me-^{iPr}PNP)CoH_2(BPin), 0.55 M in THF, 50°C, 24 h or 1 mol% of (4-Me-^{iPr}PNP)$Co(O_2CtBu)_2$, 0.55 M in THF, 80°C, 24h. Iridium: 0.1 mol % $[Ir(COD)OMe]_2$, 0.2 mol % dtbpy, 0.5 M in THF, 50°C, 24 h. (b) Cobalt: 5 mol% (4-Me-^{iPr}PNP)CoH_2(BPin), 0.55 M in THF, 50°C, 24 h. Iridium: 0.25 mol % $[Ir(COD)Cl]_2$, 0.5 mol % dtbpy, 5 mol% HBPin, 0.5 M THF, 80°C, 2 h.

Author Manuscript Author Manuscript Author Manuscript Author Manuscript

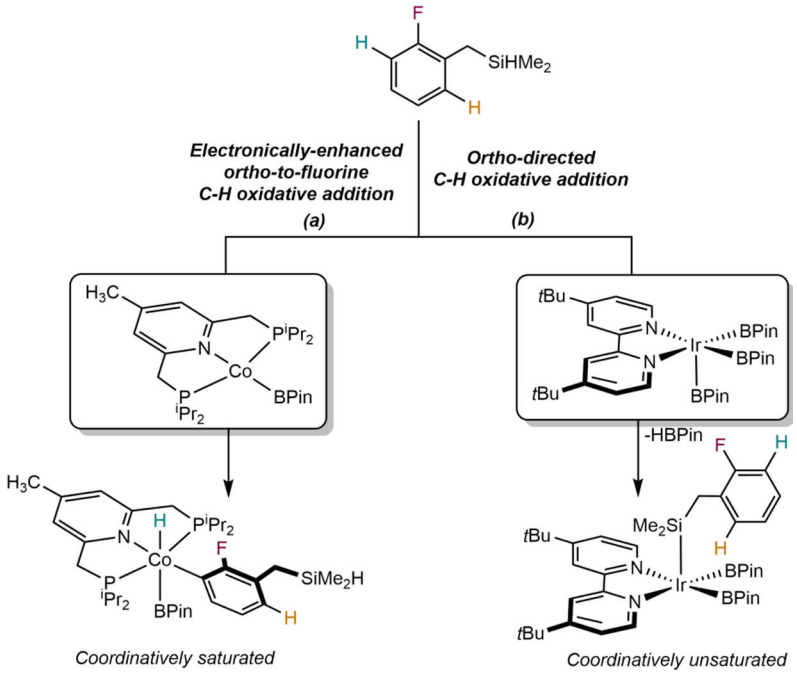

Scheme 19.

Rationale for *ortho*-to-fluorine borylation site-selectivity by cobalt catalyst and *ortho*-directed borylation by iridium catalyst (reference 104).

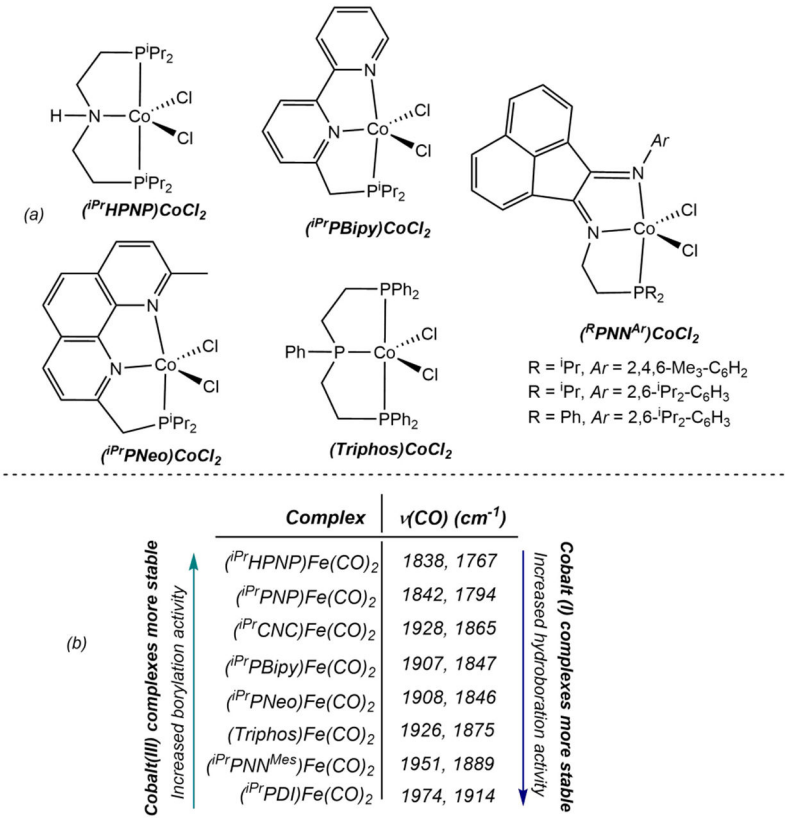

Scheme 20.

(a) Cobalt (II) dichloride precatalysts containing tridentate pincers screened for the borylation of C(sp^2)—H bonds (reference 112) and (b) νCO stretching bands of [$Fe(CO)_2$] complexes containing neutral pincer ligands (reference 112 and reference 56a for (^{iPr}CNC)$Fe(CO)_2$).

Author Manuscript Author Manuscript Author Manuscript Author Manuscript

Author Manuscript Author Manuscript Author Manuscript Author Manuscript

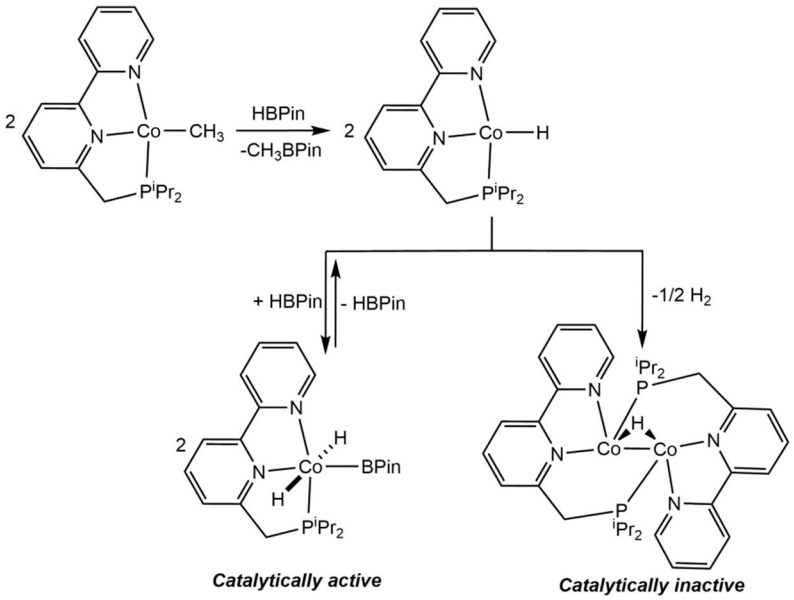

Scheme 21.

Reaction of (^{IPr}PBipy)$CoCH_3$ with excess HBPin. to form Co(III) and Co(I)-Co(0) mixed-valent complexes (reference 112).

Author Manuscript Author Manuscript Author Manuscript Author Manuscript

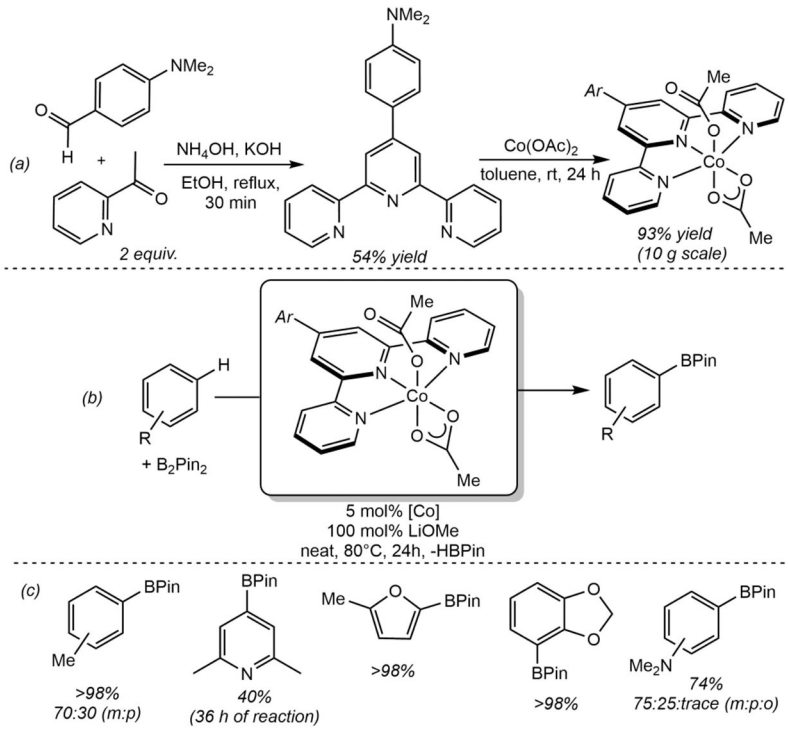

Scheme 22.

(a) Synthesis of ^{Ar}terpy and (^{Ar}terpy)Co(OAc)$_2$ on a 10 g scale and under air atmosphere (reference 111), (b) borylation of arenes and heteroarenes with B_2Pin_2 catalyzed by (^{Ar}terpy)Co(OAc)$_2$ (reference 111) and (c) selected substrate scope for borylation employing (^{Ar}terpy)Co(OAc)$_2$ as precatalyst (reference 111). Reported % numbers are isolated yields.

Author Manuscript Author Manuscript Author Manuscript Author Manuscript

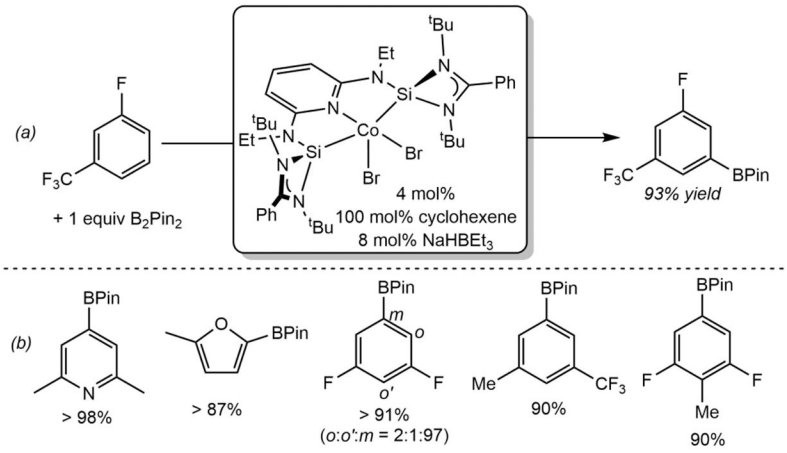

Scheme 23.

(a) Borylation of 3-fluorobenzotrifluoride by the in-situ activated (SiNSi)$CoBr_2$ precatalyst. Conditions: THF, 100°C, 24 h (reference 110) and (b) selected substrate scope for the borylation catalyzed by (SiNSi)$CoBr_2$ (reference 115). Reported % numbers are isolated yields.

Author Manuscript Author Manuscript Author Manuscript Author Manuscript

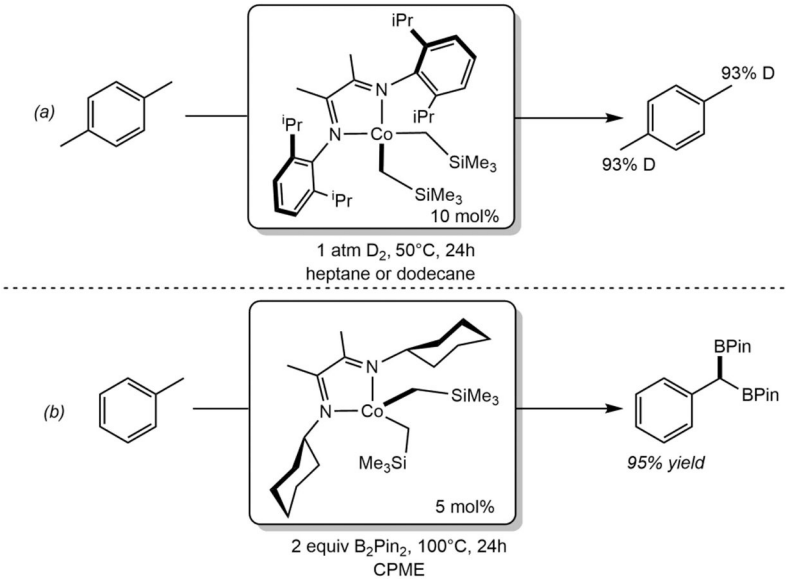

Scheme 24.

(a) HIE of the methyl groups of *para*-xylene catalyzed by (^{iPr}DI)Co(CH_2SiMe_3)$_2$ (reference 116) and (b) C(sp^3)—H benzylic diborylation of toluene catalyzed by (^{Cy}-ADI)Co(CH_2SiMe_3)$_2$ (reference 117).